LBL-31028
UC-403

Lawrence Berkeley Laboratory
UNIVERSITY OF CALIFORNIA

EARTH SCIENCES DIVISION

Transient Radial Flow to a Well in an Unconfined Aquifer, Part I: An Evaluation of Some Conceptual Methods

T.N. Narasimhan and M. Zhu

August 1991

Prepared for the U.S. Department of Energy under Contract Number DE-AC03-76SF00098

LBL--31028

DE92 009484

Transient Radial Flow to a Well in an Unconfined Aquifer, Part I: An Evaluation of Some Conceptual Methods

T. N. Narasimhan and Ming Zhu

Department of Materials Sciences and Mineral Engineering
University of California

and

Earth Sciences Division
Lawrence Berkeley Laboratory
University of California
Berkeley, California 94720

August 1991

This work was supported in part by the Director, Office of Energy Research, Office of Basic Energy Sciences, Engineering and Geosciences Division, of the U.S. Department of Energy under Contract No. DE-AC03-76SF00098.

Transient Radial Flow to a Well in an Unconfined Aquifer, Part 1: An Evaluation of Some Conceptual Models

T. N. Narasimhan and Ming Zhu

Earth Sciences Division, Lawrence Berkeley Laboratory

and

Department of Materials Science and Mineral Enginnering

University of California, Berkeley, CA 94720

ABSTRACT

The analytic solutions of Boulton (1954) and Neuman (1972) for transient flow to a well in an unconfined aquifer are based on the assumption that the role of the unsaturated zone can be adequately accounted for by restricting attention to the release of water from the zone through which the water table moves. Both researchers mathematically treat this released water as a time-dependent source term. The differences between the models of Boulton and Neuman are that the former neglects vertical components of flow in the aquifer, but allows for an exponential process for the release of water as a function of time, whereas the latter assumes instantaneous release from storage, but accounts for vertical components of flow. Given this set of assumptions, we examine the applicability of these two methods using a general purpose numerical model through a process of verification extension and comparison. The issues addressed include: the role of well-bore storage in masking intermediate-time behavior, combined effects of exponential release as well as vertical flow, logic for vertical averaging of drawdowns, and the sensitivity of system response to the magnitude of specific yield. The issue of how good the assumptions of Boulton and Neuman are in the context of the general theory of unsaturated flow is addressed in part 2 of this two-part series of reports (Zhu and Narasimhan, 1991).

1.0 INTRODUCTION

Transient analysis of radial flow of water to a well has interested groundwater hydrologists for more than half a century (Theis, 1935). Indeed Theis' classical paper applied an exponential integral solution to a water table aquifer rather than a confined aquifer, with which it was later associated. Because of the complexity of an unconfined system due to its interface with the unsaturated zone and because of the difficulties inherent in solving the unsaturated flow problem analytically, attempts have been made by many researchers to simplify the problem with idealized approximations of the effects of unsaturated zone and restrict the solution process to the saturated domain. The key feature that these idealizations must account for is the inflection frequently observed in the time-drawdown plot of unconfined aquifer pump tests. Two categories of idealizations have been used concerning the release of water from the zone through which the water table moves: (1) gradual release (Boulton, 1954) and (2) instantaneous release combined with time-dependent vertical movement of water within the aquifer (Neuman, 1972). These two widely used idealizations have been discussed by Neuman (1979).

The purpose of this paper is to investigate the applicability of these idealizations, given that the underlying assumptions regarding the role of the unsaturated zone are valid. In part 2 of this two-part series of reports (Zhu and Narasimhan, 1991), we will examine the validity of the assumptions themselves in the general context of unsaturated flow theory. We restrict consideration to the analytical models of Theis-Wenzel (Theis, 1935), Boulton (1954; 1963), and Neuman (1972; 1974). We also limit ourselves to a fully penetrating well in an aquifer with single isotropic material.

1.1 Background

A characteristic feature of an unconfined aquifer test is the inflection observed in the time-drawdown curve at intermediate times. As seen from field data presented in Figure 1, three distinct segments can be defined in the time-drawdown graph: an early-time portion coinciding with the Theis solution associated with the specific storage (S_s) of the aquifer representing the elastic component, an intermediate time portion characterized by a flattening of the curve resembling the response of a leaky aquifer, and a final portion that conforms to the Theis curve associated with the total storage ($S + S_y$), combining the effects of elastic storage and changes in saturation.

As a first approximation, one may simplify the analysis by restricting consideration to the late-time behavior of the system and use the Theis equation to assess the total storage coefficient,

$S + S_y$. Indeed, in his classical paper, Theis (1935) analyzed Wenzel's (1933) data this way. In the present work we shall call the late time Theis curve associated with $S + S_y$ the Theis-Wenzel curve.

Neglecting vertical components of flow, assuming initial hydrostatic state, and ignoring temporal changes in aquifer thickness, b, the Theis-Wenzel governing equation is given by,

$$K_r\left[\frac{\partial^2 s}{\partial r^2} + \frac{1}{r}\frac{\partial s}{\partial r}\right] = \frac{1}{b}(S + S_y)\frac{\partial s}{\partial t}, \text{ for large } t \ , \qquad (1)$$

where K_r is hydraulic conductivity in the radial direction, s is the drawdown, r is the radial distance from the axis of the pumping well, and t is time after the pumping started.

In order to interpret the drawdown behaviors at intermediate times, two categories of simplified conceptual models have been proposed. Both these models seek to account for the quantity of water that is drained vertically from the unsaturated zone to compensate for the fluid withdrawn from the system. One model assumes that water is released from storage instantaneously from the zone through which the water table moves, to be added to the top of the saturated zone and that a finite time is needed for the pressure transient effects of this addition to reach the bottom of the aquifer (Neuman, 1972; 1973; 1974; 1975). The other model assumes that water is released gradually from storage from the same zone according to an exponentially controlled delayed drainage mechanism (Boulton, 1954; 1963; 1970; Boulton and Pontin, 1971). This notion of "delayed yield" is not peculiar to unconfined aquifers. In any system (e.g., double-porosity system) with coexisting materials of strongly differing diffusivity, the low diffusivity components will cause time-lag effects (delayed yield) in the propagation of perturbations. Indeed, as pointed out by Neuman (1979), Boulton appears to have originally developed his idea for a double porosity system controlled by elastic storage and later extended it to unconfined aquifers. As a mathematically tractable approximation, Boulton suggested that the amount of water released from storage within an unconfined aquifer due to an increase in drawdown Δs during a time period from τ to $\tau + \Delta\tau$, consists of two components: (1) a volume of water instantaneously released from elastic storage per unit horizontal area, and (2) a delayed yield per unit horizontal area from the unsaturated zone to the saturated zone which, at a later time, t, is equal to $\Delta s \alpha S_y e^{-\alpha(t-\tau)}$. Here, S_y is specific yield of the aquifer, and α is an empirical constant whose reciprocal is known as the delay index. Boulton expressed the governing equation involving

delayed yield as follows (Boulton, 1954):

$$T\left[\frac{\partial^2 s}{\partial r^2}+\frac{1}{r}\frac{\partial s}{\partial r}\right]=S\frac{\partial s}{\partial t}+\alpha S_y\int_0^t\frac{\partial s}{\partial \tau}e^{-\alpha(t-\tau)}d\tau\ . \qquad (2)$$

Although in the 1954 paper Boulton did not discuss mechanisms, in his 1963 paper he indicated that delayed yield comes from above the water table. Boulton numerically estimated his analytical solution only for the case where the compressibilities of water and of the aquifer are negligible (i.e., $S_s \simeq 0$).

Almost two decades later Neuman developed an analytical solution that could produce all the three segments of the time-drawdown curve without recourse to delayed yield (Neuman, 1972; 1973; 1974; 1975). Neuman treated the unconfined aquifer as a compressible system and the water table as a moving material boundary, thus restricting attention to drainage of fluid only in the region over which the water table moves. Neuman showed that an inflection in the time-drawdown curve can also occur as a consequence of instantaneous drainage of water followed by a finite interval of time required for the drawdown perturbation to propagate from the top to the bottom of the aquifer. This effect would of course be influenced by effects of anisotropy. In this idealization, both S and S_y are constants. Later, Neuman (1974) extended his model to account for the effect of partial penetration on drawdowns. Based on the assumption of a fully penetrating line source well, Neuman expressed the governing equations as follows (Neuman, 1972):

The saturated zone:

$$K_r\left[\frac{\partial^2 s}{\partial r^2}+\frac{1}{r}\frac{\partial s}{\partial r}\right]+K_z\frac{\partial^2 s}{\partial z^2}=S_s\frac{\partial s}{\partial t}\ ,\quad 0<z<H(r,t)\ , \qquad (3a)$$

where K_r and K_z are hydraulic conductivities in the radial and the horizontal directions, and H is saturated thickness.

Initial conditions:

$$s(r,z,0)=0\ , \qquad (3b)$$

$$H(r,0)=b\ . \qquad (3c)$$

Condition on the lateral boundary:

$$s(\infty,z,t)=0\ . \qquad (3d)$$

Condition on the impervious bottom of the aquifer:

$$\frac{\partial s}{\partial z}(r, 0, t) = 0 \ . \tag{3e}$$

Conditions on the free surface:

$$K_r \frac{\partial s}{\partial r} n_r + K_z \frac{\partial s}{\partial z} n_z = \left[S_y \frac{\partial s}{\partial t} - I \right] n_z, \text{ at } (r, H, t) \ , \tag{3f}$$

$$H(r, t) = b - s(r, H, t) \ , \tag{3g}$$

where n_r and n_z are unit vectors in the radial and vertical directions, and I is vertical infiltration (recharge) rate at the water table.

Condition in the well:

$$\lim_{r \to 0} 2 \pi K_r \int_0^H r \frac{\partial s}{\partial r} dz = Q \ , \tag{3h}$$

where Q is volumetric pumping rate.

From an intuitive and qualitative view point, the Boulton idealization seems reasonable. Considering the complexity of unsaturated zone processes, the constant α parameter chosen by Boulton (as he extended his original concept) may be considered a preliminary approximation. Neuman (1979), however, takes a more focussed view of Boulton's model. He advances several arguments to show how α cannot be a constant either in space or in time. He therefore considers Boulton's model less physically sound than his own. Neuman does point out that in a model-fitting sense, either model can be used to obtain practically the same aquifer parameters except when conditions of partial penetration or anisotropy exist or when piezometer observations at specific locations within the aquifer are considered. It is worth noting that gradual desaturation of the zone through which the water table declines and gradual vertical propagation of pressure effects from the top to the bottom of the aquifer are two *independent* physical processes. In principle, both processes are likely to occur simultaneously within a dynamic unconfined aquifer.

1.2 Methodology

In the present study, we use a general purpose numerical model as a tool for verifying the three analytic solutions (Theis-Wenzel; Boulton; Neuman) and to investigate their applicability. The model chosen is TRUST (Narasimhan *et al.*, 1978), an integral finite difference algorithm for

solving multidimensional saturated-unsaturated flow problems in deformable media. To minimize spatial discretization errors in the present work, we used concepts of geometry-imbedding (Narasimhan, 1985) in discretizing the mesh in the radial direction.

2.0 SOME COMPUTATIONAL CONSIDERATIONS

2.1 Well-Bore Storage Effect

The unconfined aquifer solutions by Theis (1935), Boulton (1954), Neuman (1972) and others are restricted to treating the well as a line source. However, it is known (van Everdingen and Hurst, 1949; Papadapulos and Cooper, 1967; Agarwal *et al.*, 1970) that effects of well-bore storage may have pronounced influence on early and intermediate time-drawdown behavior.

The computational logic for simulating the well-bore is simply to treat the well as a discrete elemental volume with a capacitance, $M_{c,well}$, defined by,

$$M_{c,well} = \frac{\Delta M}{\Delta \psi} = \frac{\rho \pi r_w^2 \Delta \psi}{\Delta \psi} = \rho \pi r_w^2 \ , \tag{4}$$

where ΔM_w is the change in mass of water in the well, r_w is the well radius and $\Delta\psi$ is the change in water level. We manipulate the TRUST input in such a way that the capacitance of the well node equals $\rho \pi r_w^2$.

The well-bore storage constant, C, was defined by van Everdingen and Hurst (1949) as

$$C = \frac{1}{2}\left[\frac{\text{capacitance of well}}{\text{capacitance of a cylinder of aquifer material of volume } \pi r_w^2 b}\right]$$

$$= \frac{1}{2}\,\frac{\rho \pi r_w^2}{\rho \pi r_w^2 S_s b} = \frac{1}{2 S_s b} = \frac{1}{2S} \ , \tag{5}$$

where $S = S_s H$.

The well-bore storage constant in an unconfined aquifer decreases with time from its initial value $C_i = (2S)^{-1}$ to its final value $C_f = [2(S_y + S)]^{-1}$. The larger the C, the stronger the well-bore storage effect. Ranges of C of practical interests are provided in Agarwal *et al.* (1970). Note that C defined in this manner is independent of r_w. For a given well-bore storage constant, it is known that the effect of well-bore storage on the confined aquifer drawdown history diminishes as the distance from the pumping well or the duration of pumping increases.

2.2 Boulton's Time Convolution Integral

Consider a volume element l in a radial system which communicates with two other neighboring elements k and m. In the context of the integral finite difference method, the Boulton equation for element l is a statement of mass conservation which takes the form:

$$U_{lk}(\bar{s}_k - \bar{s}_l) + U_{lm}(\bar{s}_m - \bar{s}_l) + \rho G_l = \rho V_l \left[S_s \frac{\Delta s_{l,I}}{\Delta t_I} + \alpha \frac{S_y}{b} \int_0^{t_{I+1}} \frac{\partial s_{l,\tau}}{\partial \tau} e^{-\alpha (t_{I+1} - \tau)} d\tau \right], \qquad (6)$$

where U is the conductance between two adjoining elemental volumes, t_{I+1} is the final time at the end of the current time step Δt_I, and $\Delta s_{l,I}$ is the increase in drawdown over Δt_I. The bar over s denotes time-averaged values and G_l represents a source term.

We now examine how the integral on the right hand side may be computationally handled. The domain of integration is split into two parts: 0 to t_I and t_I to $t_I + \Delta t_I$. By assuming that the drawdown varies linearly with time during the interval Δt, the equation can be rearranged by moving the integral over the domain 0 to t_I to the left hand side. Thus,

$$U_{lk}(\bar{s}_k - \bar{s}_l) + U_{lm}(\bar{s}_m - \bar{s}_l) + \rho G_l - \rho V_l \alpha \frac{S_y}{b} \int_0^{t_I} \frac{\partial s_{l,\tau}}{\partial \tau} e^{-\alpha (t_{I+1} - \tau)} d\tau$$

$$= \rho V_l \left[S_s \frac{\Delta s_{l,I}}{\Delta t_I} + \alpha \frac{S_y}{b} \int_{t_i}^{t_{i+1}} \frac{\partial s_{l,\tau}}{\partial \tau} e^{-\alpha (t_{i+1} - \tau)} d\tau \right]$$

$$= \rho V_l \left[S_s + \frac{S_y}{b} \left(1 - e^{-\alpha \Delta t_i} \right) \right] \frac{\Delta s_{l,I}}{\Delta t_I} . \qquad (7)$$

In the numerical model, the capacitance term associated with time derivative on the right hand side of the equation is easily handled by using an effective fluid mass capacity $M_{c,\,effective} = \rho V_l [S_s + S_y(1 - e^{-\alpha \Delta t_i})/b]$, which is a function of time. The convolution integral on the left hand side can be expressed in a discretized form by summing up the amounts of water *remaining to be drained* at t_I due to the incremental drawdowns that occurred over all the previous time steps. Let t_i denote the time at the beginning of an arbitrary time step and t_{i+1} at the end. Assume that from t_i to t_{i+1} the water table in elemental volume l declines $\Delta s_{l,i}$ due to pumping. Then the *total mass of drainable water* due to this increase in drawdown is $\Delta M_{l,i} = \rho A_l S_y \Delta s_{l,i}$. By the Boulton assumption, this amount of water is not completely released over this time interval. Instead, the *actual drainage* during t_i to t_{i+1} is smaller and is given by:

$$\Delta M_{l,i}\left[1-e^{-\alpha(t_{i+1}-t_i)}\right]=\rho A_l S_y \Delta s_{l,i}\left[1-e^{-\alpha(t_{i+1}-t_i)}\right] \quad . \tag{8}$$

Hence, the mass of water *remaining to be drained* from $\Delta M_{l,i}$ is

$$\Delta M_{l,i}-\Delta M_{l,i}\left[1-e^{-\alpha(t_{i+1}-t_i)}\right]=\rho A_l S_y \Delta s_{l,i} e^{-\alpha \Delta t_i} \quad . \tag{9}$$

We now implement a computationally efficient procedure for explicitly evaluating the convolution integral on the left hand side of (7) so as to treat it as a non-linear sink term. Note that physically this quantity represents the mass of water remaining to be drained from node l at the instant t_I. Let us start with time step Δt_1, spanning the interval t = 0 to t = Δt_1. Let the incremental drawdown during this time step be $\Delta s_{l,1}$. Let $DM_{l,I}$ denote the mass of water remaining to be drained at the beginning of time step Δt_I, that is, at the instant t_I. Then, in view of (9), the mass of water remaining to be drained at the end of time step 1 (or equivalently at the beginning of time step 2) is,

$$DM_{l,2}=\rho A_l S_y \Delta s_{l,1} e^{-\alpha \Delta t_1} \quad . \tag{10}$$

We now need to evaluate the mass of water remaining to be drained at the beginning of time step 3. Note that by the end of time step 2, a portion of the mass of water given in (10) would have drained according to the exponential drainage process. Concurrently, a small amount of water will be added to the quantity in (10) due to the incremental drawdown $\Delta s_{l,2}$ that is created during time step 2. Therefore, the mass of water remaining to be drained at the beginning of time step 3 is given by:

$$DM_{l,3}=\left[DM_{l,2}+\rho A_l S_y \Delta s_{l,2}\right] e^{-\alpha \Delta t_2} \quad . \tag{11}$$

The above equation provides a simple logic to update, at the end of each time step, the mass of water that is waiting to be drained from each elemental volume in the system according to the exponential decay process assumed by Boulton. Incorporating the logic contained in (11) into (7) yields the mass conservation statement for node l during that time step:

$$U_{lk}\left[\bar{s}_k-\bar{s}_l\right]+U_{lm}\left[\bar{s}_m-\bar{s}_l\right]+\rho G_l-DM_{l,I}\left[1-e^{-\alpha \Delta t_i}\right]$$

$$=\rho V_l\left[S_s+\frac{S_y}{b}\left[1-e^{-\alpha \Delta t_i}\right]\right]\frac{\Delta s_{l,I}}{\Delta t} \quad . \tag{12}$$

2.3 Neuman's Idealization

The main feature of the Neuman idealization is that water is instantaneously drained from storage and is added at the top of the saturated zone. This water will migrate downwards as well as radially on its way to the well bore. To numerically simulate this feature, we distinguish, in writing the mass conservation equation, between an elemental volume that does not include the water table and one that does. Thus, for the elemental volume that does not include the water table, we have,

$$\sum_m U_{lm}(\bar{s}_m - \bar{s}_l) + \rho G_l = \rho V_l S_s \frac{\Delta s_l}{\Delta t} \quad . \tag{13}$$

For volume elements that include water table we can write,

$$\sum_m U_{lm}(\bar{s}_m - \bar{s}_l) = \rho V_l \left[S_s + \frac{S_y}{\Delta b'} \right] \frac{\Delta s_l}{\Delta t} \quad , \tag{14}$$

where $\Delta b'$ is the height of the elemental volume. Thus one may define an effective specific storage coefficient of $S_s + S_y/\Delta b'$ for these nodes. In the Neuman idealization, the saturated thickness of such an element, $\Delta b'$ is approximated by its initial value, Δb.

2.4 The Notion of Vertical Average

2.4.1 Mathematically Averaged Drawdown

The drawdown observed at a specific location within an unconfined aquifer is a function of radial distance, time after the start of pumping, and elevation from the base. Boulton treated drawdown to be independent of elevation, and assumed it to be only a function of r and t. Neuman, however, considered the existence of vertical flow components, and his general solution for the drawdown is expressed as s = s(r, z, t). Nontheless, Neuman also presents drawdowns averaged over the thickness of the aquifer so that s is treated as a function of r and t only. For this purpose Neuman defined the average drawdown as,

$$\bar{s}_{math}(r, t) = \frac{1}{b} \int_0^b s(r, z, t)\, dz \quad . \tag{15}$$

And when multiplied by $4\pi K b/Q$ (15) takes a dimensionless form:

$$\bar{s}_{D,math}(\beta, t_D) = \int_0^1 s_D(\beta, z_D, t_D)\, dz_D \ . \tag{16}$$

We call this a mathematical average and point out that this average is not physically meaningful because the integrand in (15) is not an additive quantity. In order that (15) be meaningful in a mass conservation sense, the integrand may be multiplied by base area and storage coefficient to yield mass of water released from storage.

2.4.2 Physically Averaged Drawdown

To be consistent with mass conservation, we may define an average drawdown on a physical basis. Intuitively one can define a physical average on the basis of capacitance as,

$$\bar{s}_{phy}(r, t) = \frac{S_y\, s(r, z=b, t) + \int_0^b S_s\, s(r, z, t)\, dz}{S_y + b S_s} \ , \tag{17}$$

and

$$\bar{s}_{D,phy}(\beta, t_D) = s_D(\beta, z_D=1, t_D) + \sigma \bar{s}_{D,math} \tag{18}$$

where $\sigma = S/S_y$.

A question may now be raised as to which of these average drawdowns a fully penetrating observation well will actually "see". Is it the mathematically averaged drawdown or the physically averaged drawdown or some other average? It appears that previous workers have assumed implicitly that it is the mathematically averaged drawdown that the fully penetrating observation well will "see". However, the reasonableness of this choice is not self-evident. Further studies are needed before this assertion can be substantiated in a credible fashion.

3.0 MODEL VERIFICATION

We use the phrase, "model verification," to denote the task of assuring internal mathematical consistency of the numerical solution before using it to investigate the applicability of unconfined aquifer analysis approaches. A well-accepted philosophy for model verification is to match, using the numerical model, known analytical solutions of special problems of interest.

3.1 Theis-Wenzel Solution

Since the Theis-Wenzel solution differs from the well-known Theis solution only in that it has an effective storage coefficient of $S + S_y$ instead of S, to verify one solution is equivalent to verifying the other. Narasimhan and Witherspoon (1976) showed that the TRUST algorithm reproduces the Theis solution (line-source solution) with acceptable accuracy.

An important extension of the line-source solution is the incorporation of the well-bore storage effect. Agarwal *et al.* (1970) developed analytical solutions giving consideration to well-bore storage effects in a well of finite diameter. Numerical results obtained for a well-bore storage constant of 100 are shown compared in Figure 2 with the analytical solution of Agarwal *et al.* (1970). It can be seen that the agreement is excellent. The volume elements (or nodes) were cylindrical shells, whose outer radii were twice the inner radii. We denote this to be a "factor 2" mesh.

3.2 Boulton Solution

The logic of treating delayed yield has been discussed in (8) through (12). In order to compare with Boulton's tabulated results (Boulton, 1963), $\sigma = S/S_y$ is chosen to be 10^{-3}. In the Boulton problem, as in the well-bore storage problem, the same factor 2 mesh was used in the verification exercise. Numerical results of dimensionless drawdowns for $\beta = 10^{-2}$ and $\alpha = 10^{-4}$, 10^{-6}, and 10^{-8} (corresponding to r/B = 1, 0.1, and 0.01) are depicted in Figure 3. Agreement with the analytical solution can be considered very good. The slight differences noticed at early times are attributable to minor well-bore storage effects.

3.3 Neuman Solution

The main features of the Neuman idealization are: instantaneous drainage, line source well, existence of vertical flow components and constant thickness of the saturated zone. The role of specific yield is modeled as a source term at the water table.

For purposes of verifying the numerical model, a hypothetical case, as first suggested by Cooley (1971) and later used by Neuman (1972), was considered. The input parameters used are given in Table 1.

Table 1. Input parameters for the Cooley problem*

b (m)	r_w (well radius) (m)	K (m/s)	S_s (m^{-1})	S_y	σ	Q m^3/sec
18.14	0.128	7.073×10^{-4}	1.969×10^{-3}	0.23	0.155	1.5×10^{-3}

*Solutions are compared at r = 12.52 m, for which $\beta = 0.477$.

Neuman's analytical solution was evaluated by a program, DELAY2 (Neuman, 1989). In order to conform to the analytical solution, the well was treated as a line source. As suggested by Narasimhan (1985), the line source well was simulated by locating the nodal point of the volume element representing the well at 0.60653 r_w, where r_w is the radius of the innermost node. A factor 2 mesh, as shown in Figure 4 was used. Vertical flow was considered by discretization in the vertical direction. From bottom to top, the aquifer was discretized into seven 2 m-thick layers, two 1 m-thick layers, and one 2.14 m-thick layer. The 2.14 m thick uppermost layer was specified to have an effective specific storage coefficient of ($S_s + S_y/2.14$) in accordance with (14). The pumping rate was chosen such that the water table will not fall below this layer. Other layers of the aquifer were specified a constant specific storage coefficient of S_s.

Results obtained with the numerical simulator TRUST are compared with those from DELAY2 for point drawdowns at $z_D = 0$ and $z_D = 0.855$ (Figure 5a) and for mathematically averaged drawdowns of Neuman (Figure 5b). Note that at large times the effective storage coefficient is merely the sum of elastic storage coefficient (S) and specific yield (S_y), and all drawdowns fall on the Theis-Wenzel curve associated with ($S + S_y$). Good agreement between numerical and analytical results for both point solutions and mathematical average drawdowns verifies the internal consistency of the TRUST code.

4.0 APPLICABILITY OF MODELS

4.1 The Goal

The unconfined aquifer hydraulics topic has been discussed in detail by Neuman (1979) and Gambolati (1976). The purpose of this study is to provide some additional insights by starting with the existing analytic solutions and going a little beyond, using a general purpose numerical model. Specifically, we address the following issues which are relevant to evaluating the applicability of the models of Boulton and Neuman:

- How limiting is the line-source assumption? How much will the early time and intermediate time behaviors be masked by well-bore storage effects?
- Are delayed drainage and vertical flow mutually exclusive? If they can occur simultaneously, how will they influence pressure transient response?
- What rationale should one use in vertically averaging drawdowns in an unconfined aquifer?
- Because of the combined effects of well-bore storage and radial distance, how will the duration of the intermediate time behavior be abridged?
- How sensitive is the unconfined aquifer pressure transient behavior to the magnitude of specific yield?

4.2 The Boulton Model

4.2.1 Well-bore Storage Effect

The results of numerical simulations including well-bore storage effect in the Boulton model are presented in Figures 6a and 6b. Figure 6a pertains to observations at the well-bore (r_w = 0.128 m) and Figure 6b pertains to a location somewhat further away at r = 0.2 m. The results clearly demonstrate that the well-bore storage effect on drawdowns close to the well is strong. Note that for an unconfined aquifer the well-bore storage parameter changes with time. The initial value of well-bore storage constant is $C_i = (2 S_s b)^{-1}$ and the final value $C_f = [2 (S_s b + S_y)]^{-1}$. In this case $C_i = 5000$ and $C_f = 5$.

In general, the drawdown versus time curve at early times will be dictated by the well-bore storage effect, while at later times the curve will converge to the Theis-Wenzel solution. Figures 6a and 6b show that, in the presence of well-bore storage effect, the Boulton solution developed for the intermediate range of times is so severely masked that it is of little practical use.

4.2.2 Delayed Yield in Conjunction with Vertical Flow

Although Boulton used the delayed yield concept and Neuman considered vertical flow components, it stands to reason that these two processes are not mutually exclusive and that they occur simultaneously in an unconfined aquifer. We therefore conduct a numerical experiment in which these two effects are combined.

The combination of the Boulton delayed yield constant and vertical flow was realized by using a two-dimensional mesh (Figure 4). The following input parameters were used: $\sigma = 10^{-3}$, $\beta = 1.56 \times 10^{-4}$, and $\alpha = 10^{-4}$. The results, with and without the effect of vertical flow, are shown compared in Figure 7.

It is seen that the vertical flow components increase drawdown noticeably during intermediate times. For the particular set of parameters considered, consideration of vertical flow leads to larger drawdowns than those obtained with Boulton solution for $t_D > 10^2$. Also, while the Boulton model suggests that the Theis-Wenzel solution can be used for $t_D \geq 10^5$, Figure 7 indicates that consideration of vertical flow delays it significantly.

4.3 The Neuman Model

In investigating the applicability of the Neuman idealization, we look into the effects of averaging process, the influence of radial distance on vertical flow components, effect of well-bore storage, and effect of decreasing saturated thickness. Sensitivity of solutions to the value of specific yield is also studied.

4.3.1 Effect of Well-bore Storage on Pumping Well Drawdown

The well-bore storage effect on drawdown observed in the pumping well is illustrated in Figures 8a and 8b for two values of σ: $\sigma = 10^{-1}$ and $\sigma = 10^{-4}$. The well radius is chosen to be 12.8 cm, a value reasonably typical of water wells and oil wells.

At early times the drawdown curve for the well is characterized by a unit slope and deviates significantly from the Theis curve. At intermediate times the well drawdown curve approaches, but never coincides with the early Theis curve because of time-dependent storage coefficient. The curve converges to the Theis-Wenzel solution after the delayed yield ceases to influence the drawdowns and the unconfined aquifer behaves effectively like an aquifer with constant storativity. Comparison of Figures 8a and 8b indicates that this meeting point is delayed when σ is

decreased. That is, the smaller the specific storage, the longer the time over which the discrepancy between the well-bore storage solution and the line-source solution is noticeable.

The effect of well-bore storage in unconfined aquifer response has generally been neglected in the groundwater literature. Our study suggests that this effect cannot be ignored in dealing with unconfined aquifers because it could significantly mask a large part of the intermediate time behavior predicted by the analytical solution, for example, up to $t_{D,w} = 10^3$ for $\sigma = 10^{-1}$ and up to $t_{D,w} = 5 \times 10^5$ for $\sigma = 10^{-4}$. In a recent paper, Ramey *et al.* (1989) have stressed the importance of well-bore storage effects on unconfined aquifer flow (gravity-drained systems) based on data from petroleum reservoirs.

4.3.2 Effects of Averaging Procedure

The physically averaged and the mathematically averaged drawdowns defined in section 2.4 are contrasted in Figure 9a for the case of $\sigma = 10^{-1}$ and in Figure 9b for $\sigma = 10^{-4}$. In both cases the well radius is arbitrarily set to be 10 mm to reasonably approximate a line source, the original saturated thickness is 15.651 m, the hydraulic conductivity is 3.6×10^{-4} m/s, the specific yield is 0.23, and the pumping rate is 1.5×10^{-3} m^3/s. The drawdowns at r = 0.1b ($\beta = 0.01$) are presented. In Figure 9a the initial well-bore storage constant C_i is 21.7 and the final value C_f is 1.98, and in Figure 9b $C_i = 2.17 \times 10^4$ and $C_f = 2.17$.

It is seen that the curve for the physically averaged case is markedly different from that for the mathematically averaged case. At early times the physically averaged drawdown deviates from the Theis solution associated with S_s, while at late times it converges to the Theis-Wenzel curve associated with $(S + S_y)$. Comparing the numerical with the analytical results of physically averaged as well as mathematically averaged drawdowns, Figure 9a shows that when C_i is small (21.7) the well-bore effect is negligible, and that the numerical results agree very well with the analytical results. However, when C_i is increased to 2.17×10^4 in Figure 9b, the well-bore effect on the numerical results of mathematically averaged drawdown at early times becomes very strong, whereas the physically averaged drawdowns (at later times) are not affected.

The remarkable difference between the mathematically averaged and the physically averaged drawdowns as displayed in Figures 9a and 9b raises an interesting question: Which averaging procedure will provide drawdowns agreeing with the drawdowns "seen" by an observation well? We suspect that the use of mathematical average is an arbitrary choice, perhaps motivated merely by computational simplicity. It seems that some justifiable logic is needed to choose

between different averaging procedures.

4.3.3 The Role of Time-Dependent Saturated Thickness

As pumping continues and the water table declines, the saturated thickness of the aquifer will diminish with time. In his analytical approach, Neuman (1972; 1974) ignored the effects arising due to the time dependence of saturated thickness.

We investigated the reasonableness of this assumption by taking into account the change in the saturated thickness and the associated change in the conductances between elemental volumes. It is to be expected that this effect on drawdown will become more pronounced as drawdown increases in relation to the total saturated thickness due to increased pumping rate. For the same aquifer with $\sigma = 10^{-1}$, the drawdown of water level in the pumping well is plotted versus time in Figures 10a and 10b, respectively, for a pumping rate of 10^{-2} and 2.5×10^{-2} m^3/s.

It is seen that as the saturated thickness and the transmissivity decrease with increased pumping, the drawdown in the pumping well is increased. For the particular combination of parameters studied, when the pumping rate is 10^{-2} m^3/s and the water table has only dropped by some 15% of the initial saturated thickness, the numerically evaluated drawdown does not deviate considerably from the analytical solution (Figure 10a). However, for the same well and the same aquifer, when the pumping rate is 2.5 times higher and the water table has dropped by 30% b, the effect becomes much stronger after $t_D \gg 10^2$ and the discrepancy between the analytical and numerical results has increased to as much as 16%.

4.3.4 Effect of Radial Distance on Point Drawdowns

We have already seen that well-bore storage effects mask early time and intermediate time responses. Now since all solutions converge on to the Theis-Wenzel curve, it is clear that under field conditions in which strong well-bore storage effects will be the rule rather than an exception, the distinctive signatures in pressure transient response stemming from Neuman's solution will be limited to a restricted band or window in the time domain. We now proceed to gain some insights into the size of this time band.

Shown in Figures 11a, 11b and 11c are the drawdown-time plots for three radial distances: $\beta = 0.01$, 0.16, and 0.64 ($r = 0.03$ b, 0.4 b, and 0.8 b). In each figure, well-bore solutions with change in saturated thickness taken into account are contrasted against line-source solutions based on the Neuman assumptions for two vertical locations: $z_D = 0$ and 0.799. The following

parameters are used: $\sigma = 10^{-4}$, $S_y = 0.23$, $S_s = 1.47 \times 10^{-6}\ m^{-1}$, b = 15.651 m, $K = 3.6 \times 10^{-4}$ m/s and $C_f = 2.17$. For the particular combination of parameters, it is found that the "time-window" extending from the time the well-bore storage solution joins the Neuman solution to the time at which the Neuman solution merges with the Theis-Wenzel solution, varies from about 1.8 log cycles for r = 0.1b ($\beta = 0.01$) to 2.4 log cycles for r = 0.8b ($\beta = 0.64$).

4.3.5 Sensitivity to Specific Yield

We now examine the effect of the magnitude of specific yield on the Neuman solution. In order to study the sensitivity of drawdown to the value of specific yield, for the same set of parameters we decreased the specific yield by a factor of 2 in one additional run. We also decreased the specific storage coefficient by the same factor so that σ remains constant. The resultant drawdown-time plot is presented in Figure 11d for radial distance r = 0.4b ($\beta = 0.16$). Compared to Figure 11b it is seen that Neuman's line-source solution is not changed (because σ is constant), whereas the well-bore solution is changed. This is because in the numerical solution the (final) well-bore storage constant is directly related to the specific yield as $C_f = [2(S_y + S)]^{-1} = [2S_y(1 + \sigma)]^{-1}$. When the specific yield is decreased by a factor of 2 (Figure 11d), the final well-bore storage constant is increased by a factor of 2 to 4.34, the well-bore effect lasts longer than in Figure 11b, as also the time after which the Theis-Wenzel solution is valid. Thus, Figures 11b and 11d clearly show that as the specific yield decreases, well-bore storage effect lasts longer and the Neuman solution is useful for analysis only over about 1.1 log cycles of time as opposed to 2.0 log cycles for $S_y = 0.23$. Stated differently, it is clear from Figures 11a through 11d that in the presence of well-bore storage the Neuman solution is of practical interest only over a finite "window" in the time domain. Table 2 summarizes the size of these windows for Figures 11a through 11d. The width of this window noticeably decreases with decreasing the specific yield.

4.4 Comparison of the Boulton Model and the Neuman Model

The numerical results for the Boulton problem are shown compared with those of Neuman's mathematically averaged drawdowns for $\beta = 0.01$ and 2.56 in Figures 12a and 12b, respectively. Figure 12a shows the results for $\alpha = 10^{-4}$ and 10^{-6} (corresponding to r/B = 1 and 0.1), and Figure 12b shows for $\alpha = 10^{-4}$ and 10^{-6} (r/B = 16 and 1.6). σ is 0.001 in both figures.

It is seen that Neuman's curve falls in an envelope bounded by Boulton's solution for a range of α values, which suggests that Neuman's solution can be matched to a particular case of

Table 2. Size of window in the time domain over which the Neuman solution is valid ($\sigma = 10^{-4}$).

S_y	β	Δt_D (log cycles)
0.23	0.01	1.8
0.23	0.16	2.0
0.23	0.64	2.4
0.115	0.16	1.1

Boulton's solutions. Indeed, Gambolati (1976) pointed out that the two analytical solutions can be reconciled by defining α as a function dependent in some complex way on r, b, K_r/K_z, S_y, and t. However, it is necessary to recognize that making such direct comparison of the two solutions is merely a mathematical exercise lacking physical significance since one model is established by assuming instantaneous drainage and the other assuming delayed yield, which are treated as mutually exclusive. Furthermore, Figure 12a also indicates that at a given location (r/b = constant), in order to let the Neuman solution agree with the Boulton solution, $K_D = K_z/K_r$ can be adjusted in the Neuman solution so that the required value of $\beta = K_D(r/b)^2$ can be obtained. In other words, vertical anisotropy is a mathematical parameter available for adjustment in the Neuman model, whether anisotropy physically exists or not.

5.0 DISCUSSION

Both Boulton and Neuman consider the zone through which the water table moves as the source of drained water. They however differ on the mechanism by which the drained water finds its way to the saturated zone. In this paper we address two issues related to the models of Boulton and Neuman: their practical utility and their physical realism.

In practice, both models are capable of imitating the intermediate time behavior of drawdown data from unconfined aquifer tests but with the help of very different model parameters. In this sense, the advantage of the Neuman model over the Boulton model is that the former can account for effects of partial penetration as a well as anisotropy.

A serious limitation that is common to both models stems from the assumption of neglecting well-bore storage effects. Open wells with a fluctuating water level, which are typical of wells in unconfined aquifers, contribute to large well-bore storage effects on pressure transients. Simulations carried out as part of the present study involving parameters reasonably typical of unconfined aquifers suggest that all of the early-time effects and a significant portion of the intermediate time signatures of Boulton' solution and Neuman's solutions will be masked by well-bore storage effects. Specifically, it appears that when specific yield is large, the Neuman signatures may be discernible only over about 2 log cycles of time for relatively large values of specific yield. When specific yield is smaller, this time window may shrink to one log cycle of time or less. We also found well-bore storage effects to be important for partially penetrating wells.

In order to simplify the mathematical solution, it is common practice to average drawdowns or potentials in the vertical direction. In heterogeneous media under transient conditions the task of averaging drawdowns or potentials must go hand in hand with the purpose for which the averaging is desired. The way Neuman has formulated the problem, the capacitance of the aquifer (i.e., storativity) is a function of elevation. At the upper surface of the aquifer storativity includes the effects of specific yield, whereas S_y is zero elsewhere. In this sense the aquifer is heterogeneous. Presumably, one would vertically average drawdown in aquifer under the assumption that an observation well fully penetrating the well will in fact respond with the defined predicted average. The manner in which Neuman averages drawdown vertically in the aquifer ignores vertical variations in storativity and hence is not mass-conserving. Numerical experiments with a mass-conserving averaging scheme suggest a very different drawdown pattern. It is suggested that averaging of potentials in a transient heterogeneous system requires much additional study.

Granting the assumption that consideration of the zone through which the water table moves is adequate to account for the effects of the unsaturated zone, the issue of physical realism of either model is not well-assured. Delayed yield and vertical flow are not mutually exclusive processes. They could indeed exist concurrently. It seems likely that effects of delayed yield could be parametrized with the help of anisotropy and vice versa. Consequently, it is perhaps more relevant to consider how either model could be practically used to analyze field problems in a model-fitting sense and to use such parameters to make predictions with the self-same model than to consider the relative merits of the physical processes.

NOTATION

A	base area, m^2
b	initial saturated thickness of aquifer, m
B	$= \sqrt{T/(\alpha S_y)}$
C	well-bore storage constant
C_i	initial well-bore storage constant of unconfined aquifer
C_f	final well-bore storage constant of unconfined aquifer
H	saturated thickness
k	absolute permeability, m^2
K	hydraulic conductivity, m/s
K_D	$= K_z/K_r$, dimensionless hydraulic conductivity
K_r	radial hydraulic conductivity, m/s
K_z	vertical hydraulic conductivity, m/s
M_c	fluid mass capacity or capacitance, kg/m
n	porosity
Q	volumetric pumping rate, m^3/s
r	radial distance from center of pumping well, m
$\bar{r}$	location of radial nodal point, m
s	drawdown of hydraulic head, m
s_D	$= 4\pi Kbs/Q$, dimensionless drawdown
$\bar{s}$	average drawdown, m
$\bar{s}_{math}$	mathematically averaged drawdown, m
$\bar{s}_{phy}$	physically averaged drawdown, m
$\bar{s}_{D,math}$	dimensionless mathematically averaged drawdown, m
$\bar{s}_{D,phy}$	dimensionless physically averaged drawdown, m
S	$= S_s b$, storage coefficient
S_r	residual saturation, dimensionless
S_s	specific (or elastic) storage, m^{-1}
S_y	$= n\,(1 - S_r)$, specific yield
t	time, s
t_D	$= Kt/(S_s r^2)$, dimensionless time with respect to S
t_y	$= Kt/((S_y/b)r^2)$, dimensionless time with respect to S_y
t_t	$= Kt/((S_s + S_y/b)r^2)$, dimensionless time with respect to $S + S_y$
T	$= K\,b$, transmissivity or transmissibility, m^2/s
U_{lm}	conductance of interface between l and m, kg/m-s
V_l	fluid volume of aquifer subregion l, m^3
z	vertical distance from bottom of aquifer, m
z_D	$= z/b$, dimensionless vertical distance
α	reciprocal of Boulton's delay index, s^{-1}
β	$= K_D r^2/b^2$

ψ pressure head, m
ρ density of water, kg/m^3
σ = S/S_y

Acknowledgments

We thank Shlomo Neuman for providing the program DELAY2. We also thank Kenzi Karasaki and Ron Falta for reviewing the manuscript. This work was partly supported by the U. S. Department of Energy under Contract Number DE-AC03-76SF00098.

RERERENCES

Agarwal, R. G., R. Al-Hussainy and H. J. Jr. Ramey, An investigation of wellbore storage and skin effect in unsteady liquid flow: I. Analytical treatment, *Soc. Pet. Eng. J., 249*, 279–290, 1970.

Boulton, N. S., Unsteady radial flow to a pumped well allowing for delayed yield from storage, General Assembly of Rome, Tome II, *Publ. 37, Inst. Ass. Sci. Hydrol.*, 472–477, 1954.

Boulton, N. S., Analysis of data from non-equilibrium pumping tests allowing for delayed yield from storage, *Proc. Instn. Civil Eng., 26*, 469–482, 1963.

Boulton, N. S., Analysis of data from pumping tests in unconfined anisotropic aquifers, *J. Hydrol., 13* (10), 369–378, 1970.

Boulton, N. S. and J. M. A. Pontin, An extended theory of delayed yield from storage applied to pumping tests in unconfined anisotropic aquifers, *J. Hydrol., 14* (1), 53–65, 1971.

Cooley, R. I., A finite difference method for unsteady flow in variably saturated porous media: Application to a single pumping well, *Water Resour. Res., 7* (6), 1607–1625, 1971.

Freeze, R. A. and J. A. Cherry, *Groundwater*, Prentice-Hall, 1979.

Gambolati, G., Transient free surface flow to a well: An analysis of theoretical solutions, *Water Resour. Res., 12* (1), 27–39, 1976.

Kroszynski, U. I. and G. Dagan, Well pumping in unconfined aquifers: The influence of unsaturated zone, *Water Resour. Res., 11* (3), 479–490, 1975.

Narasimhan, T. N., Geometry-imbedded Darcy's law, *Water Resour. Res., 21* (8), 1285–1292, 1985.

Narasimhan, T. N. and P. A. Witherspoon, An integrated finite difference method for analyzing fluid flow through porous media, *Water Resour. Res., 12* (1), 57–63, 1976.

Narasimhan, T. N., P. A. Witherspoon and A. L. Edwards, Numerical model for saturated-unsaturated flow in deformable porous media, Part II: The algorithm, *Water Resour. Res., 14* (2), 255–261, 1978.

Neuman, S. P., Theory of flow in unconfined aquifers considering delayed response of the water table, *Water Resour. Res., 8* (4), 1031–1045, 1972.

Neuman, S. P., Supplementary comments on 'Theory of flow in unconfined aquifers considering delayed response of the water table,' *Water Resour. Res., 9* (4), 1102–1103, 1973.

Neuman, S. P., Effect of partial penetration on flow in unconfined aquifers considering delayed response, *Water Resour. Res., 10* (2), 303–312, 1974.

Neuman, S. P., Analysis of pumping test data from anisotropic unconfined aquifers considering delayed response, *Water Resour. Res., 11* (2), 329–342, 1975.

Neuman, S. P., Perspective on 'delayed yield,' *Water Resour. Res., 15* (4), 899–908, 1979.

Neuman, S. P., DELAY2 computer program, *Personal Communication,* 1989.

Papadapulos, I. S. and H. H. Cooper, Jr., Drawdown in a well of large diameter, *Water Resour. Res., 3* (1), 241–244, 1967.

Ramey, H. J., G. Lichtenberger and H. J. Davitt, Well test analysis for gravity drainage systems, *SPE No. 890017,* 1989.

Theis, C. V., The relationship between the lowering of the piezometric surface and the rate and duration of discharge of a well using groundwater storage, *Trans. Am. Geophys. Union, 16,* 519–524, 1935.

van Everdingen, A. F. and W. Hurst, The application of the Laplace transformation to flow problems in reservoirs, *Trans. Am. Inst. Min. Metall. Pet. Eng., 186,* 305–324, 1949.

Wenzel, L. K., Specific yield determined from a Thiem's pumping-test, *Trans. Am. Geophys. Union, 14,* 475-477, 1933.

Zhu, M. and T. N. Narasimhan, Transient radial flow to a well in an unconfined aquifer: A testing of hypotheses, *LBL-31029,* 1991.

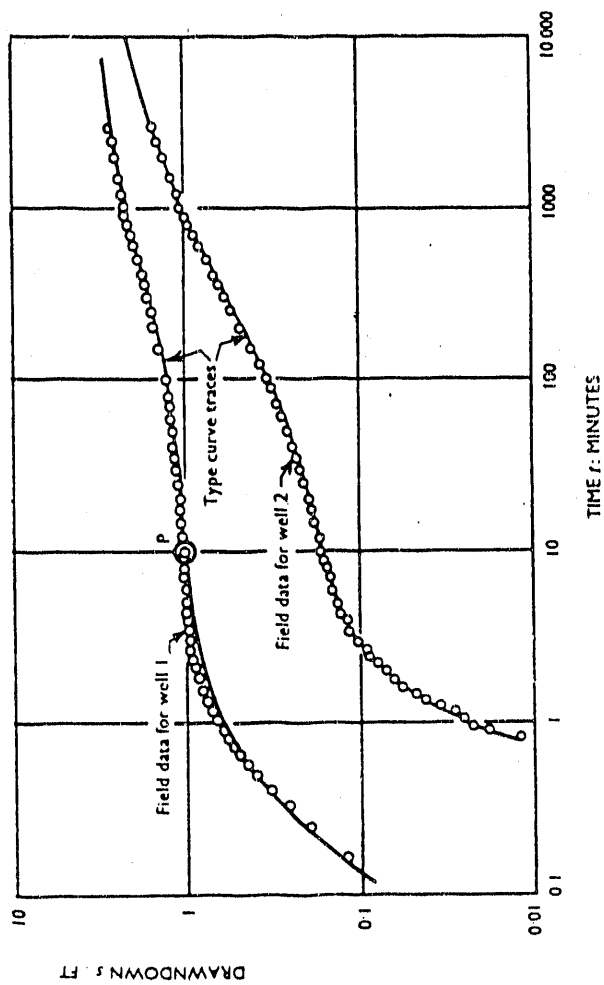

Fig. 1. Drawdowns observed in an unconfined aquifer pumping test (after Boulton, 1963).

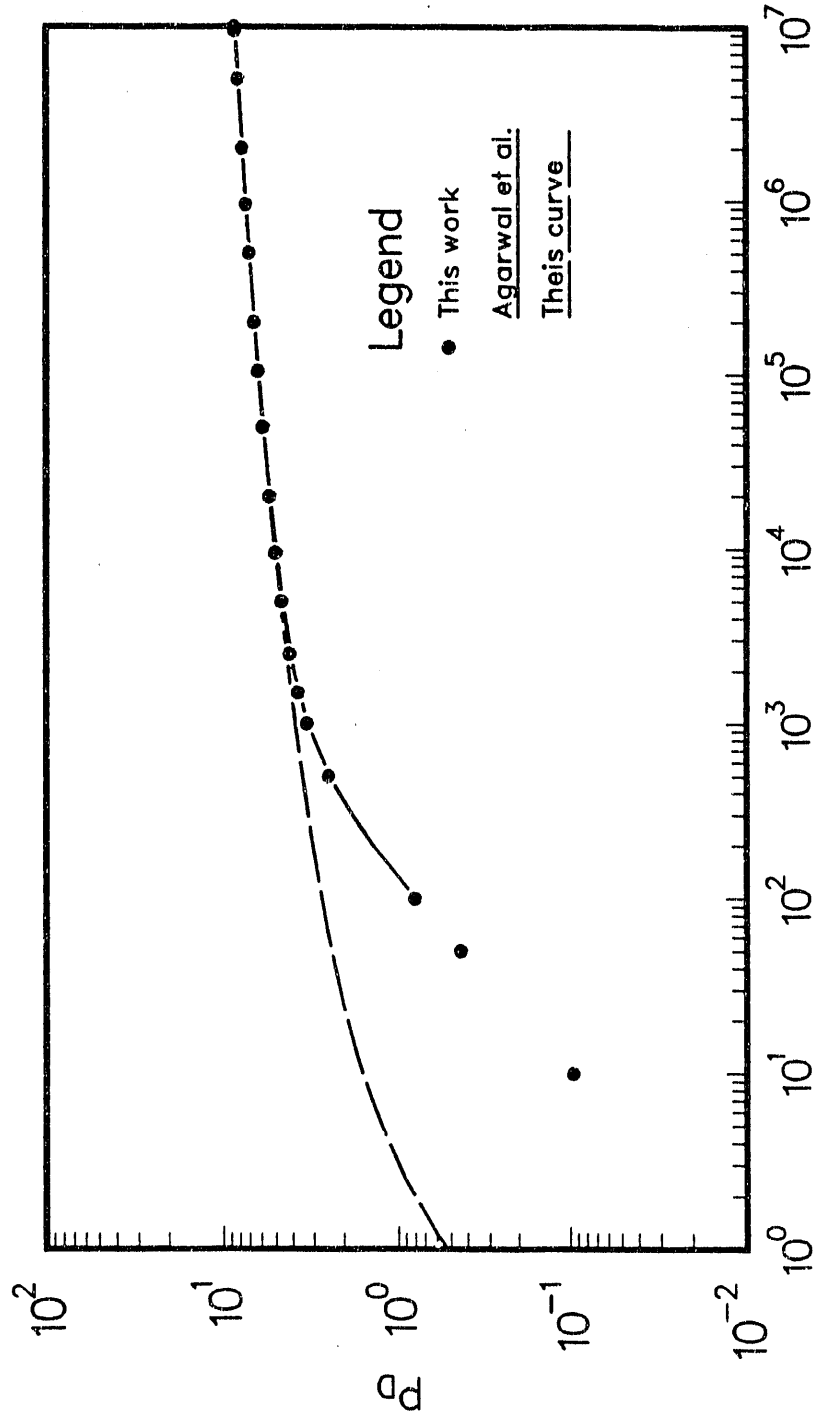

Fig. 2. Wellbore storage effect: Comparison with Agarwal et al.'s and Theis' analytical solutions. $r_w = 1$ mm, $C = 100$

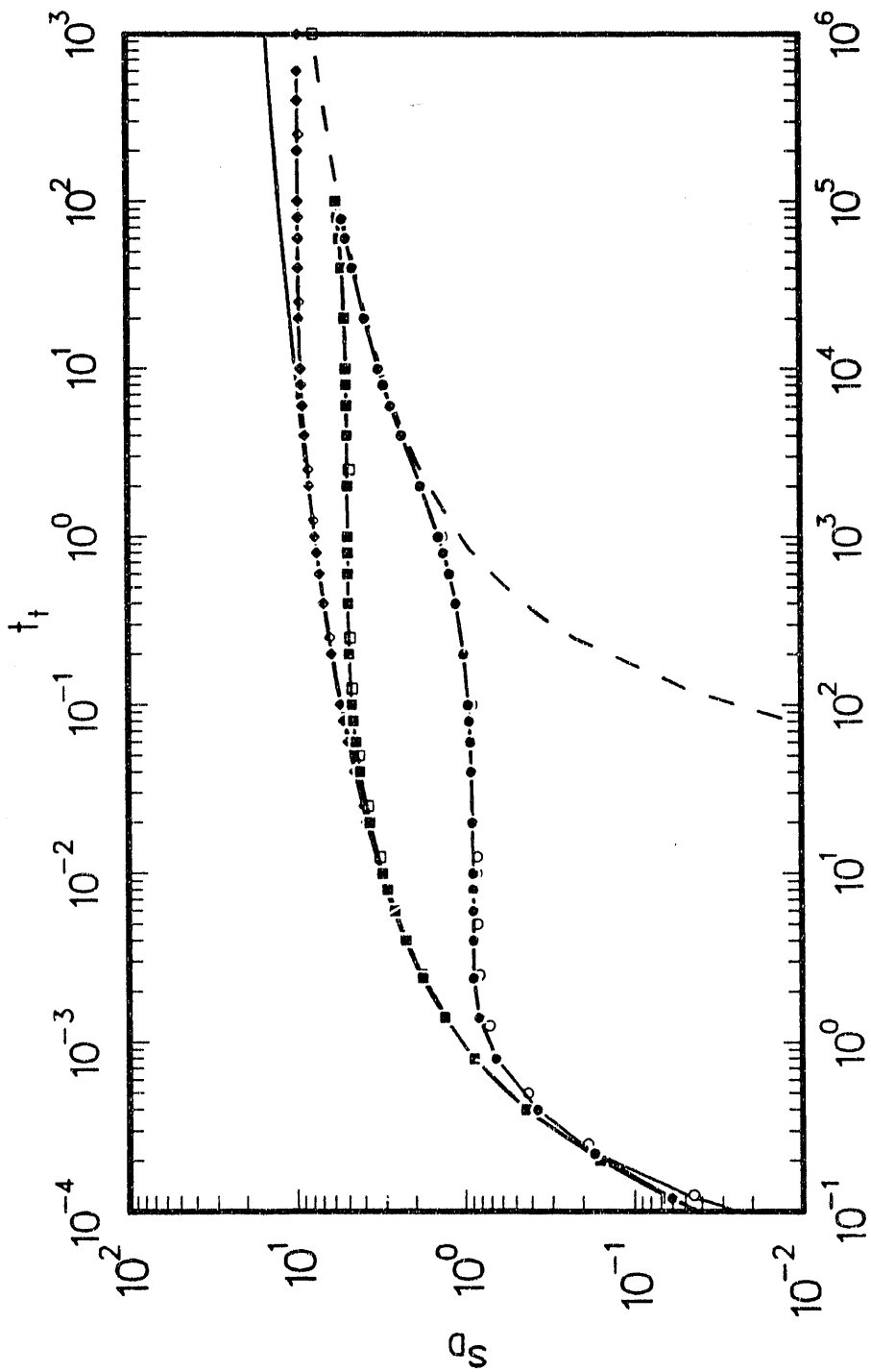

Fig. 3. Comparison with Boulton's analytical results: σ=0.001, β=0.01

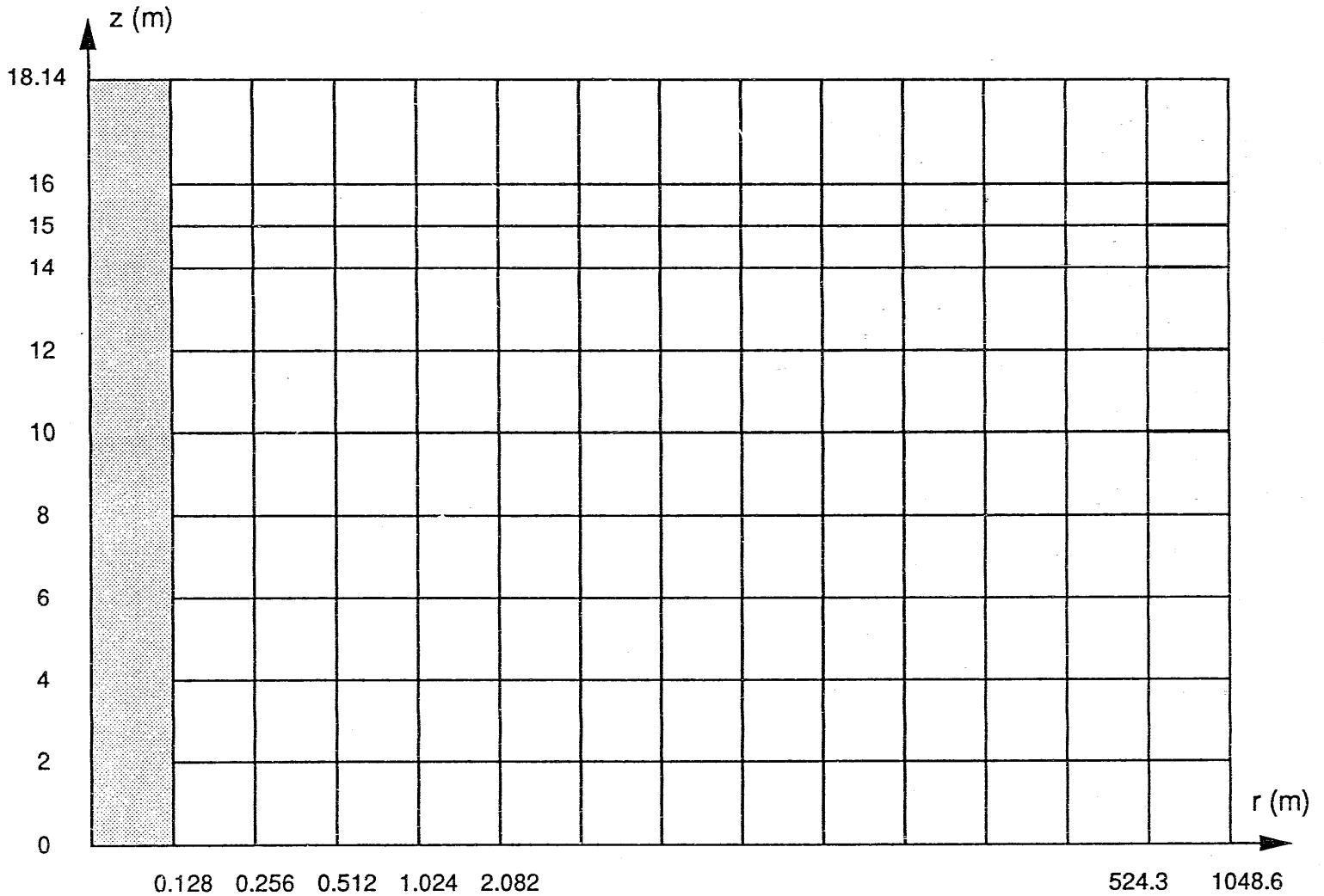

Fig. 4. The cylindrical mesh used in numerical simulation of the Cooley problem. Not to scale in the radial direction.

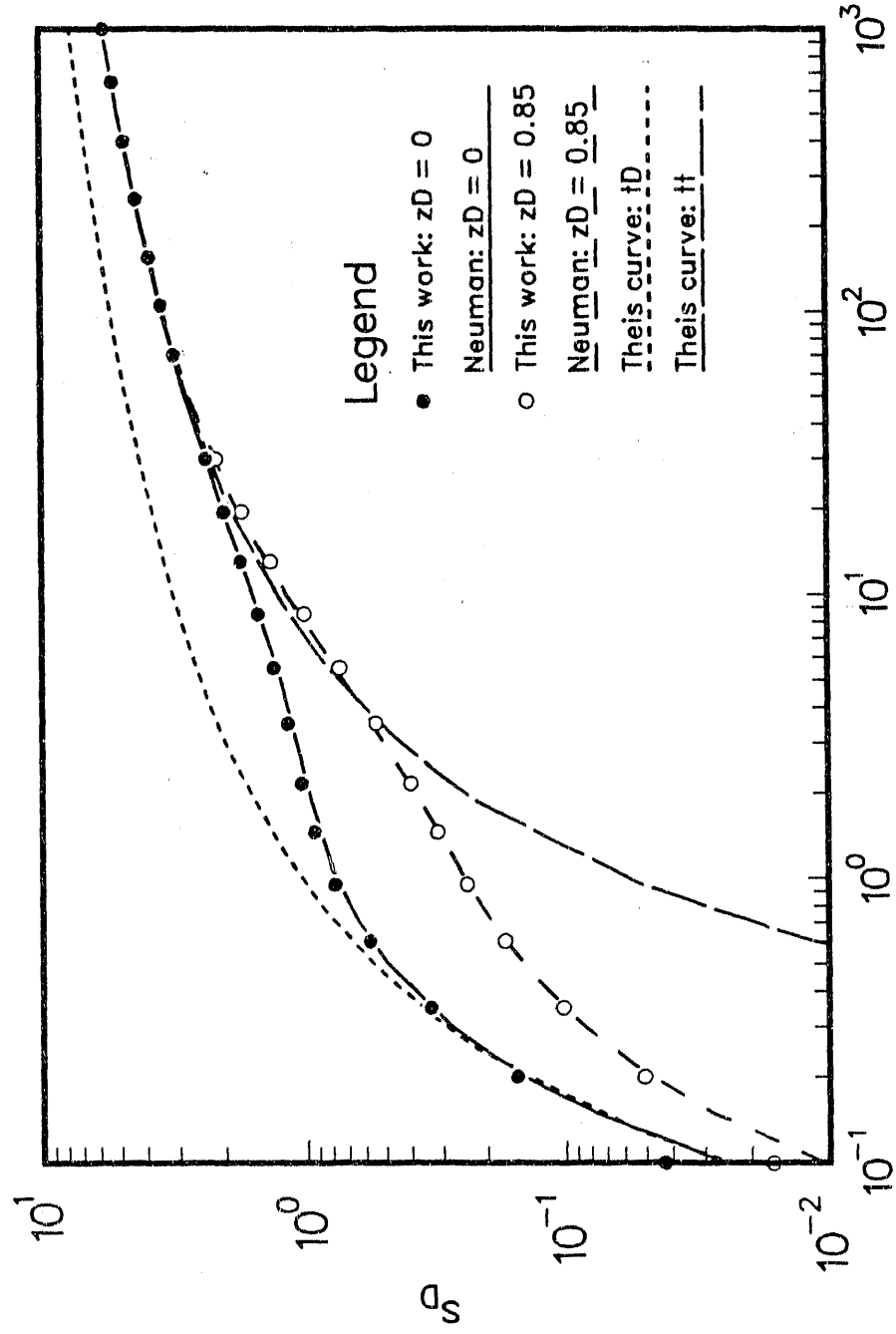

Fig. 5a. Comparison with Neuman's analytical results for point drawdown: $\sigma = 0.155$, $\beta = 0.477$.

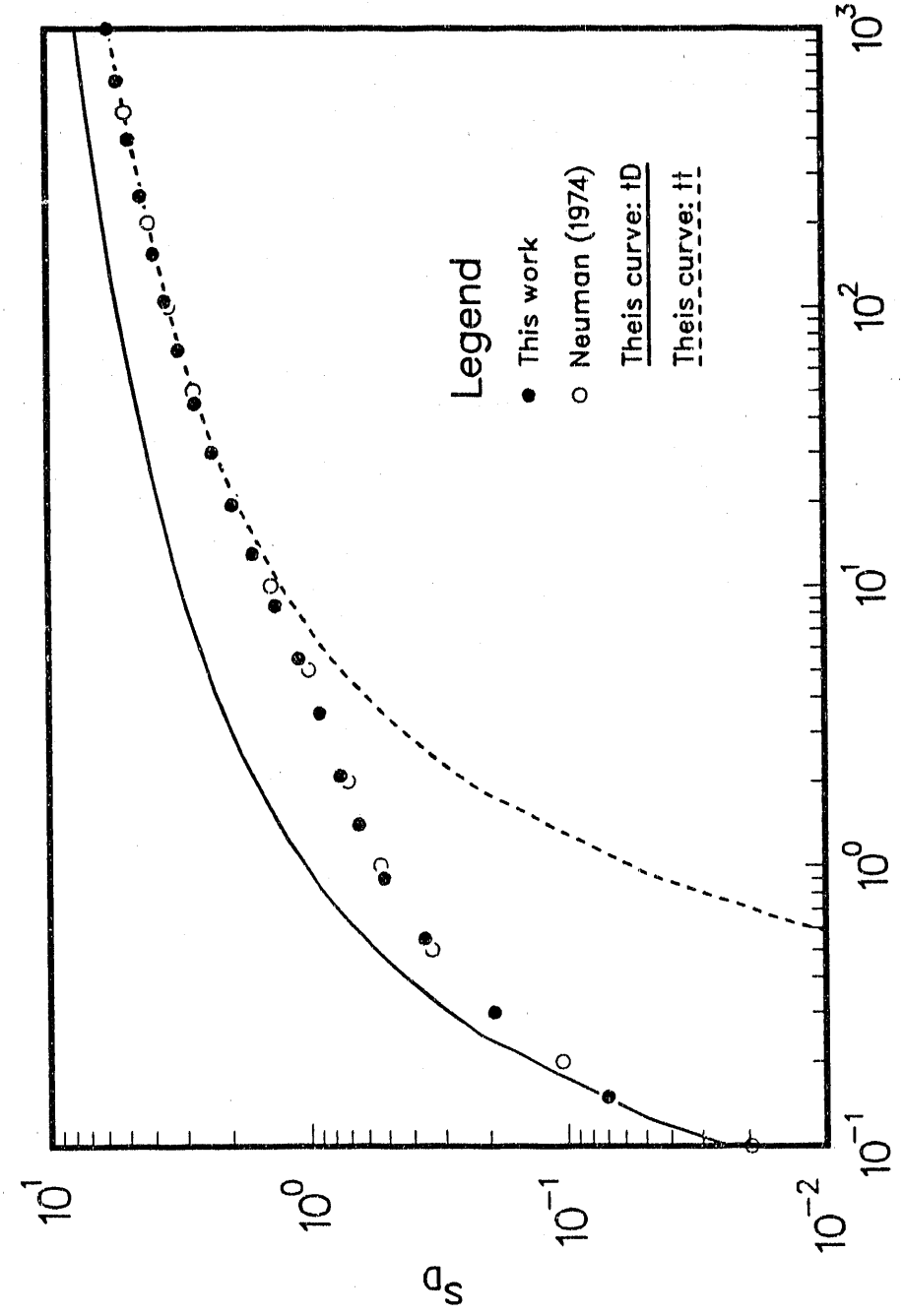

Fig. 5b. Comparison with Neuman's analytical results for mathemathically averaged drawdown: $\sigma = 0.155$, $\beta = 0.477$.

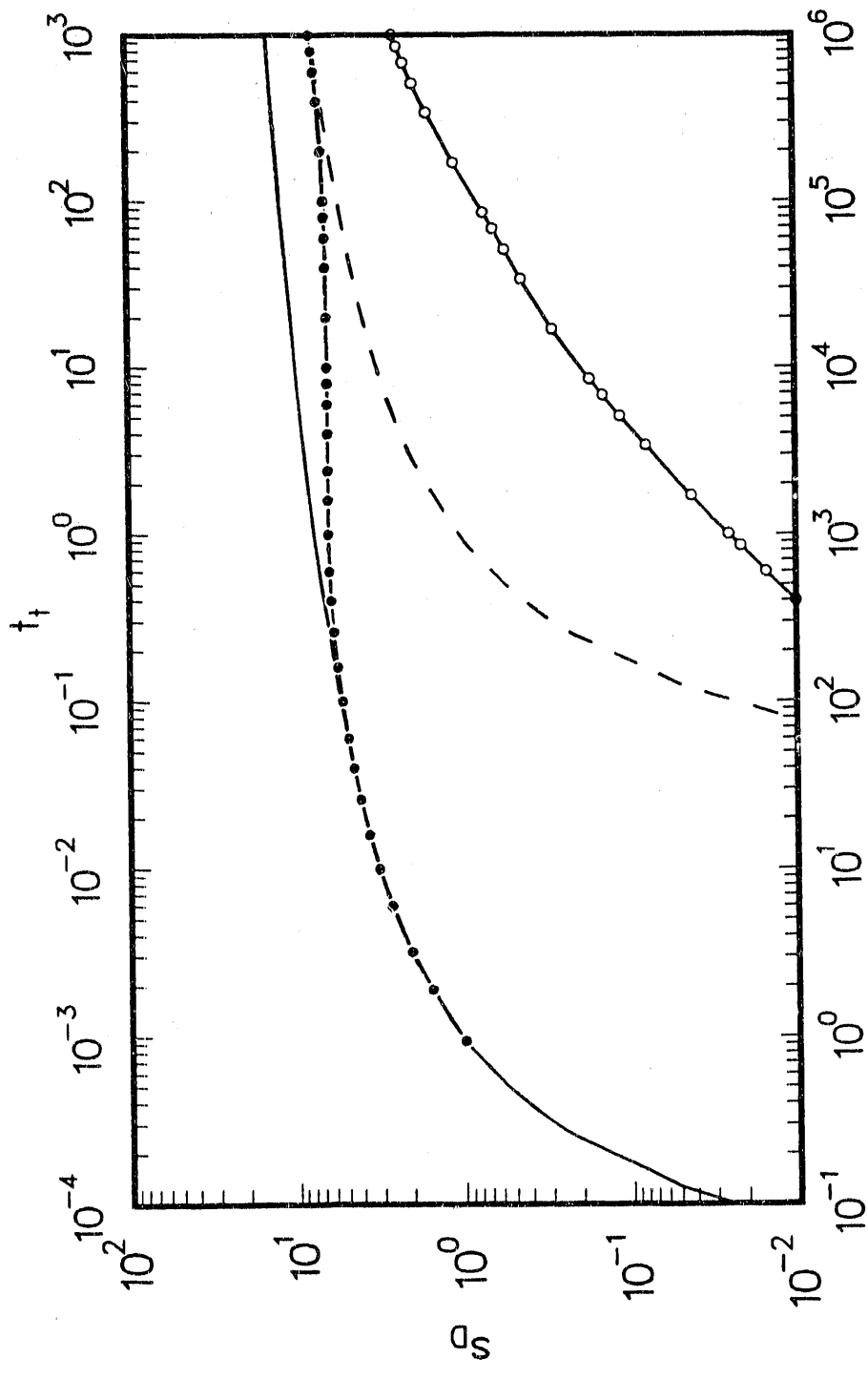

Fig. 6a. Boulton problem: Wellbore storage effect included.
σ = 1E−3, r_w = 1.28E−1 m, β_w = 6.69E−5, r/B = 8.18E−3.

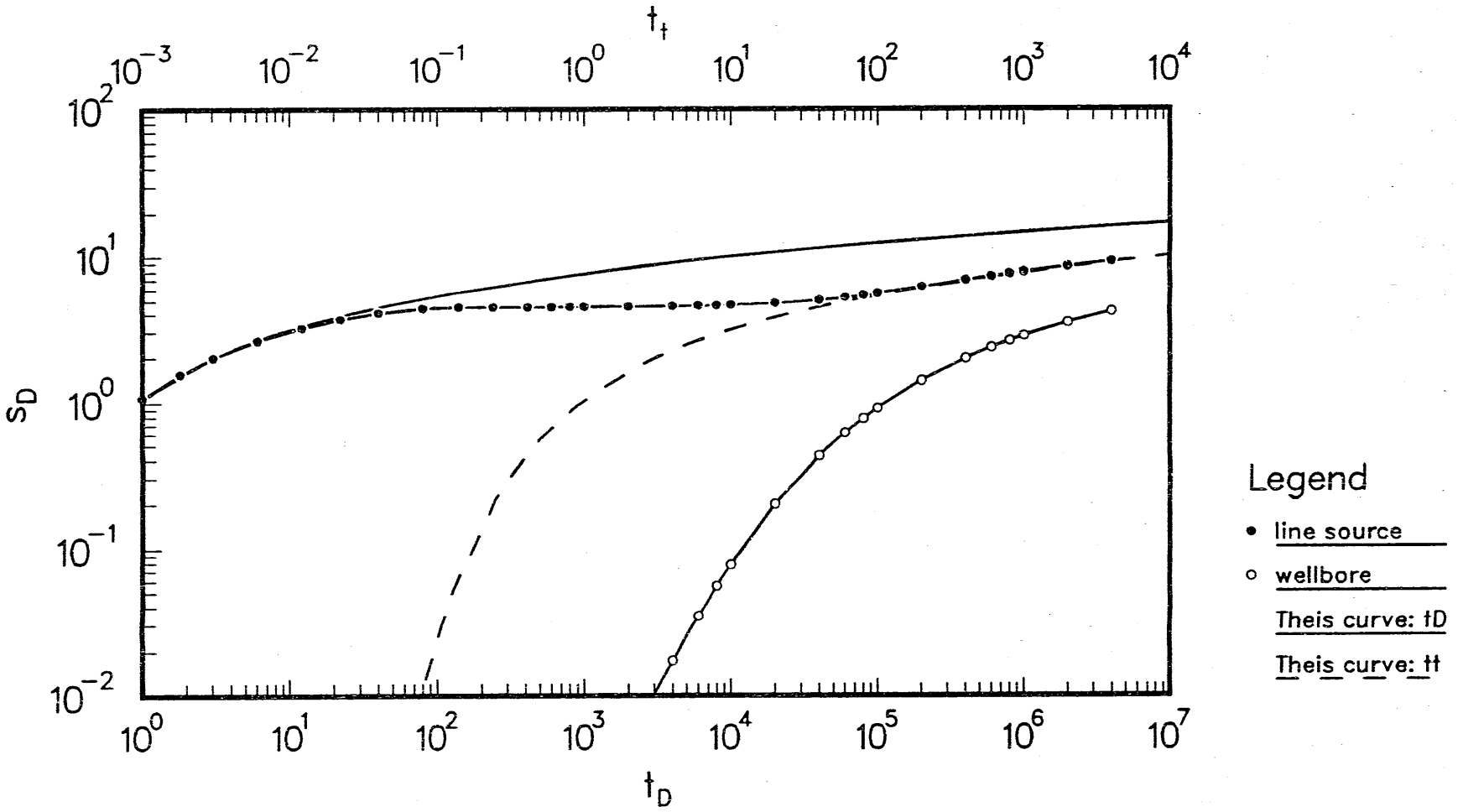

Fig. 6b. Boulton problem: Wellbore storage effect included.
σ = 1E−3, r_w = 1.28E−1 m, β = 1.56E−4, r/B = 1.25E−1.

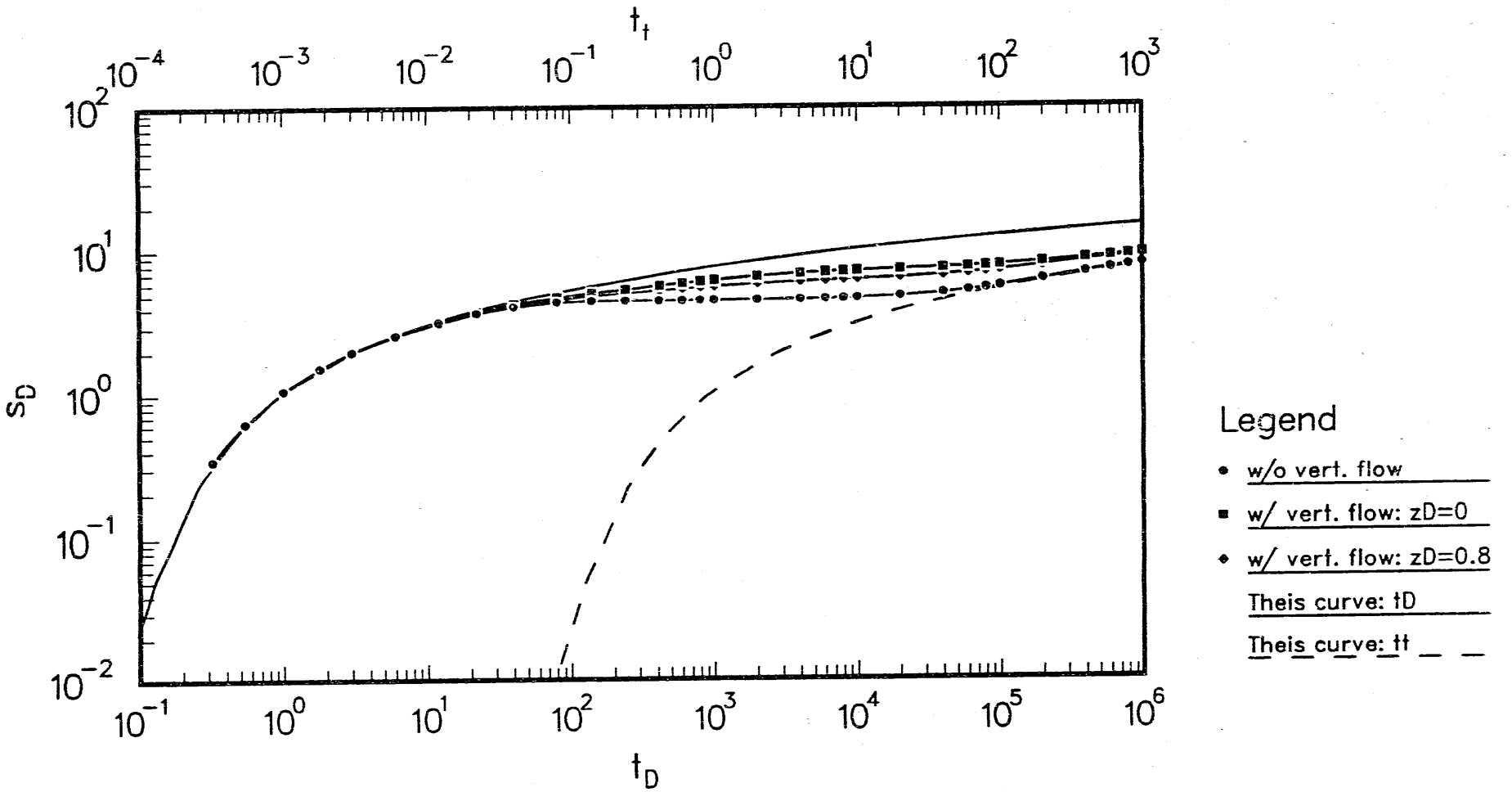

Fig. 7. Boulton problem: Effect of vertical flow included.
σ = 1E−3, r_w = 1.28E−1 m, β = 1.56E−4, r/B = 1.25E−1.

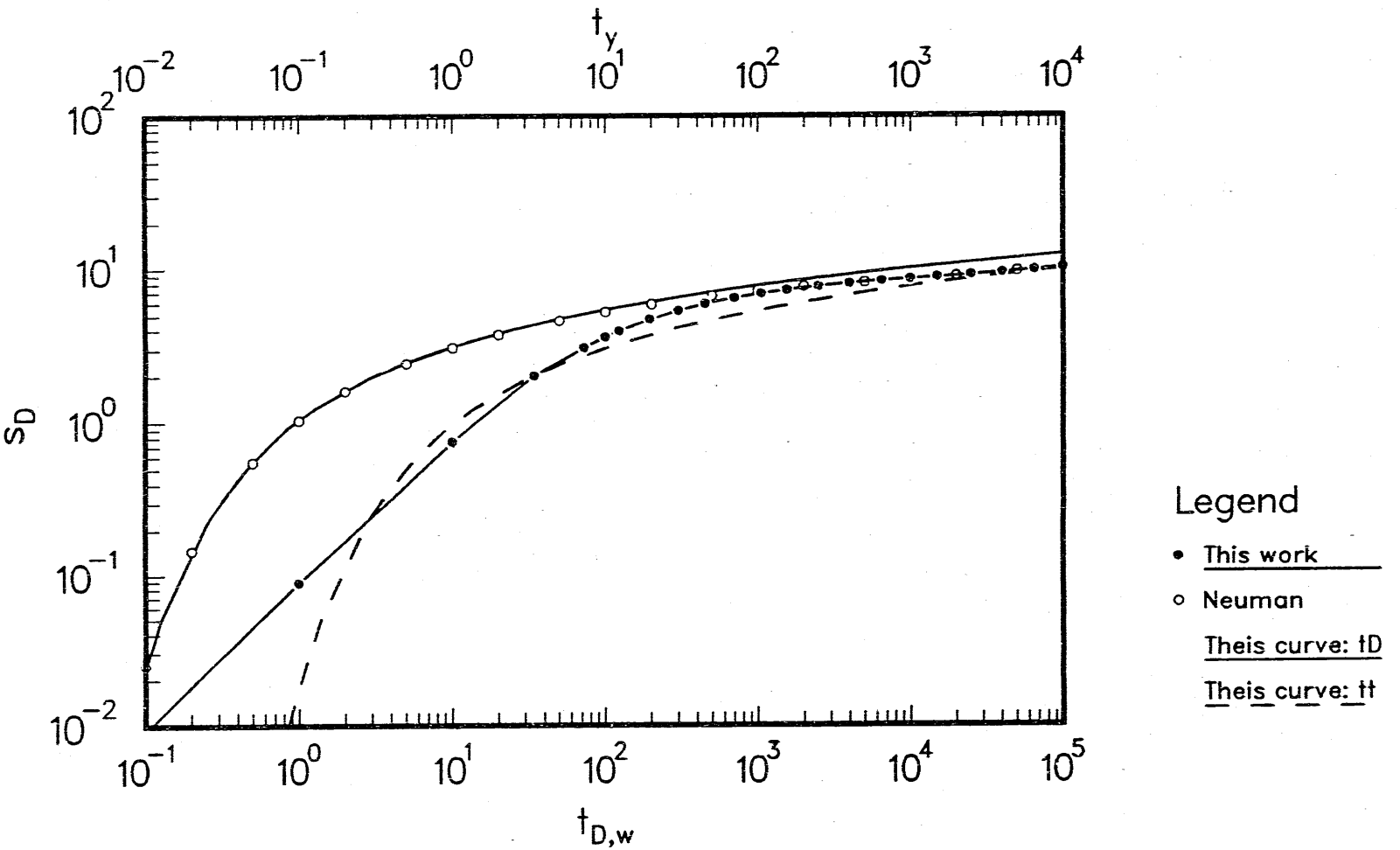

Fig. 8a. Neuman problem: Effect of wellbore storage.
r_w = 0.128 m, β_w = 6.69E−5, σ = 0.1.

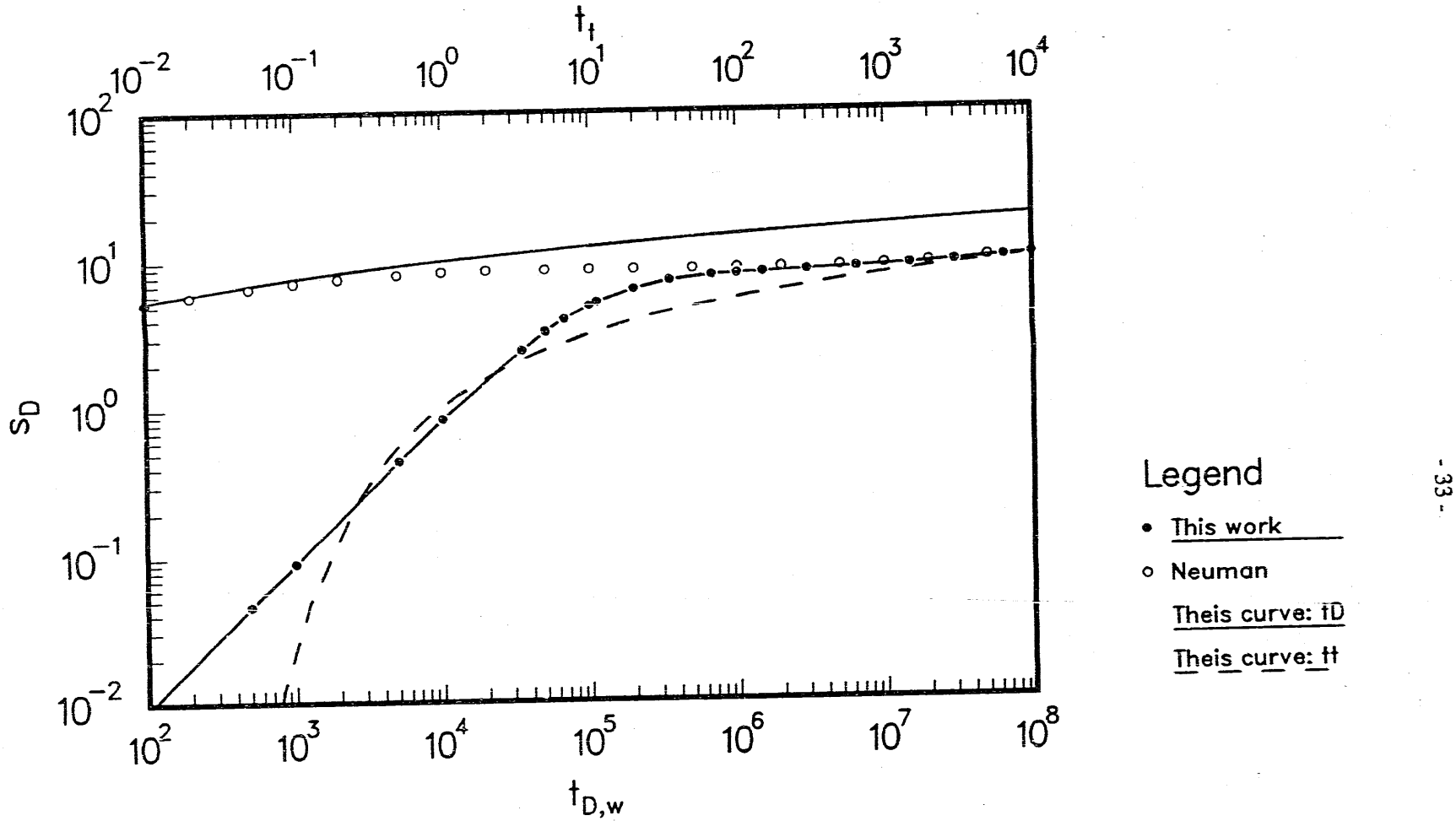

Fig. 8b. Neuman problem: Effect of wellbore storage.
$r_w = 0.128$ m, $\beta_w = 6.69E{-}5$, $\sigma = 0.0001$.

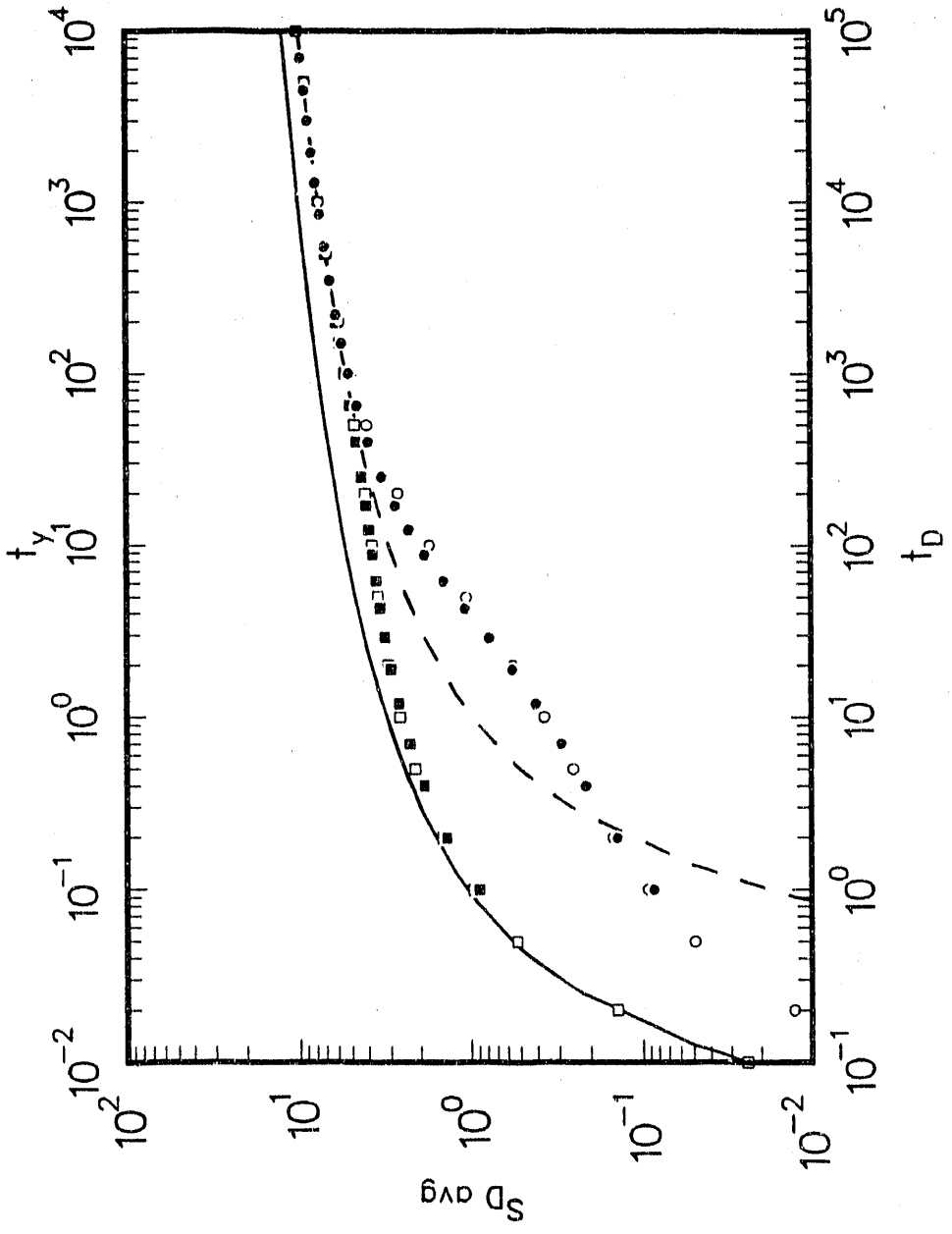

Fig. 9a. Neuman problem: Comparison between mathematical and physical averages. $\sigma = 0.1$, $\beta = 0.01$.

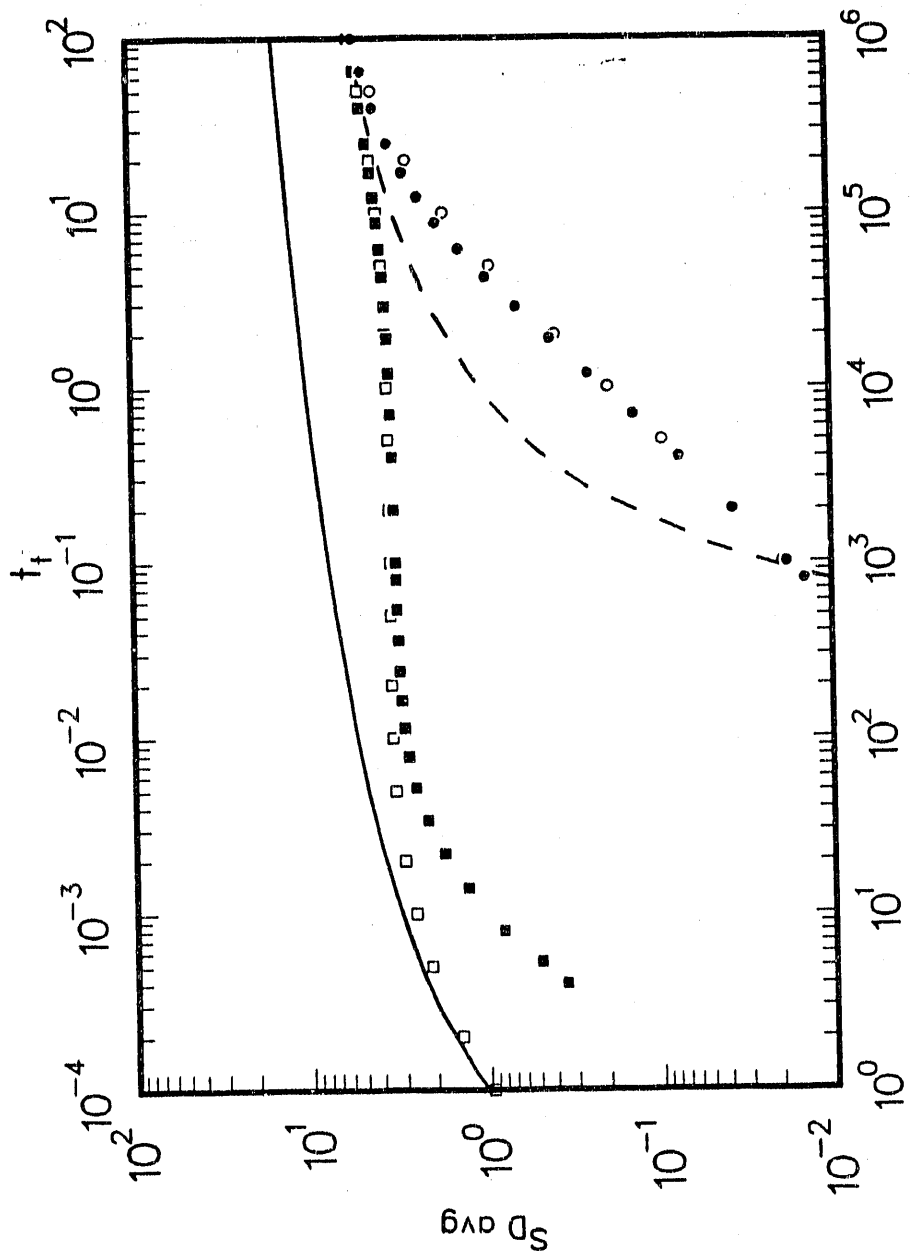

Fig. 9b. Neuman problem: Comparison between mathematical and physical averages. $\sigma = 0.0001$, $\beta = 0.01$.

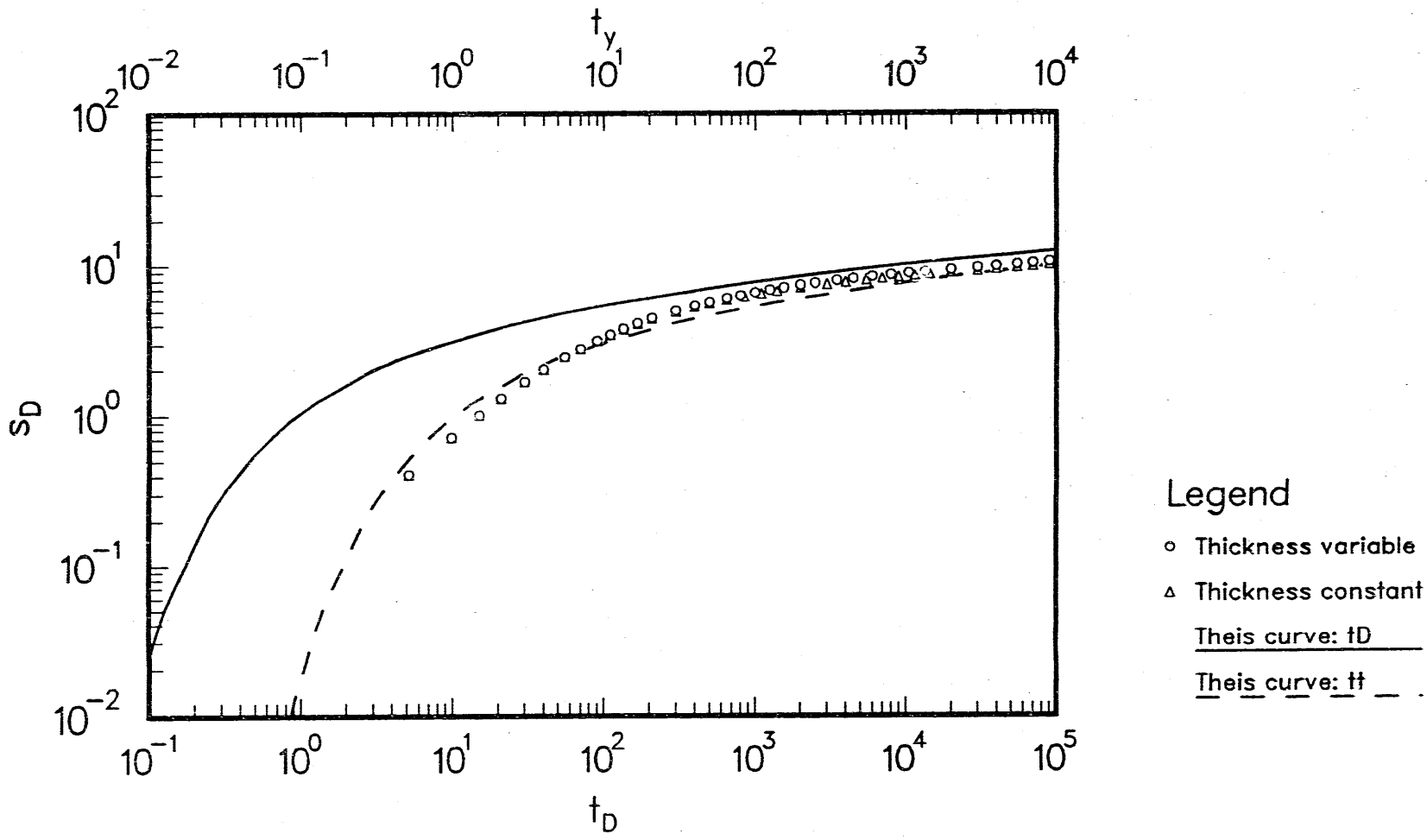

Fig. 10a. Neuman problem: Effects of decreasing saturated thickness.
$\sigma = 0.1$, $\beta_w = 6.69E{-}5$, $Q = 1E{-}2$ m^3/s.

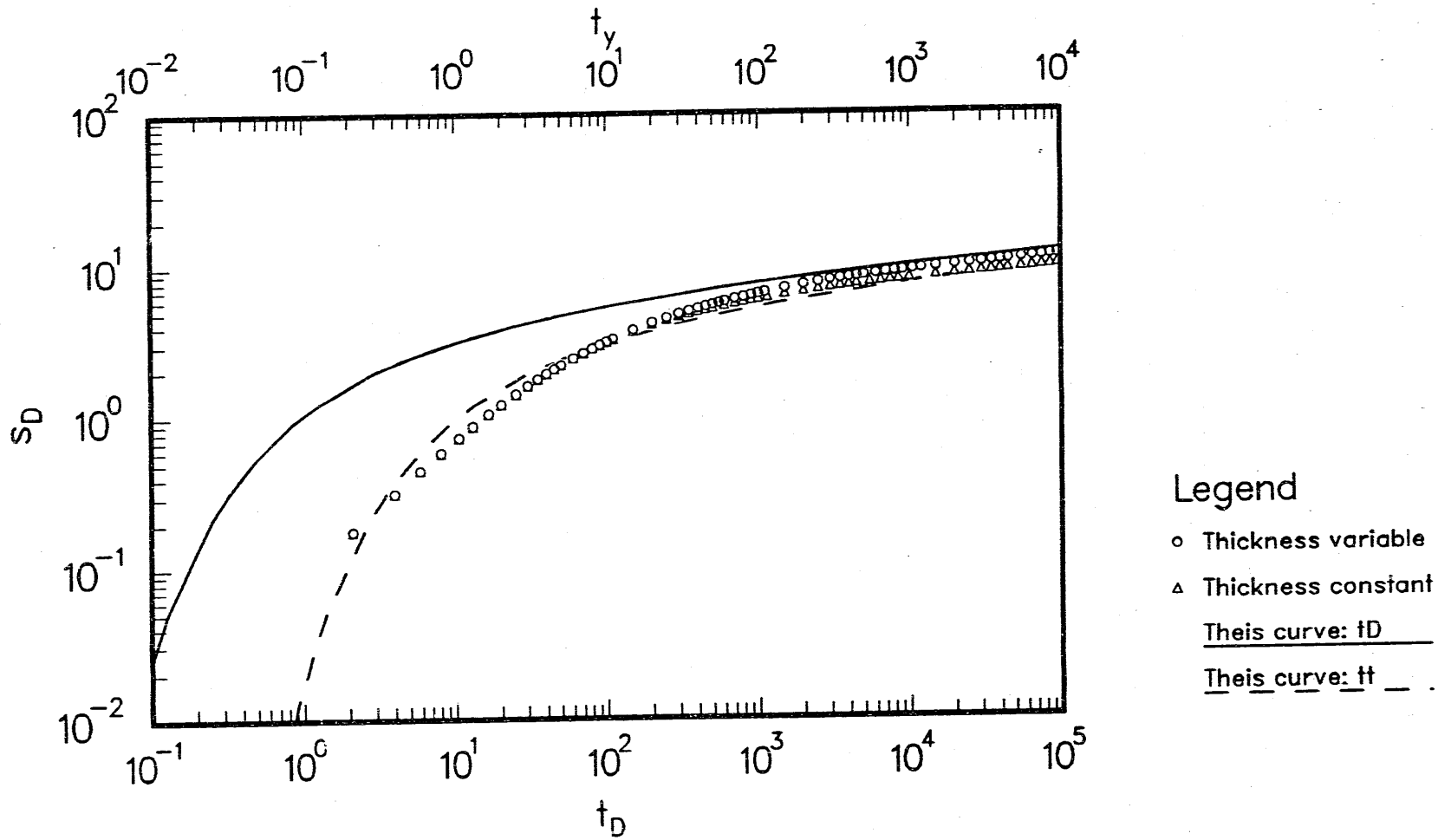

Fig. 10b. Neuman problem: Effects of decreasing saturated thickness.
$\sigma = 0.1$, $\beta_w = 6.69E{-}5$, $Q = 2.5E{-}2$ m^3/s.

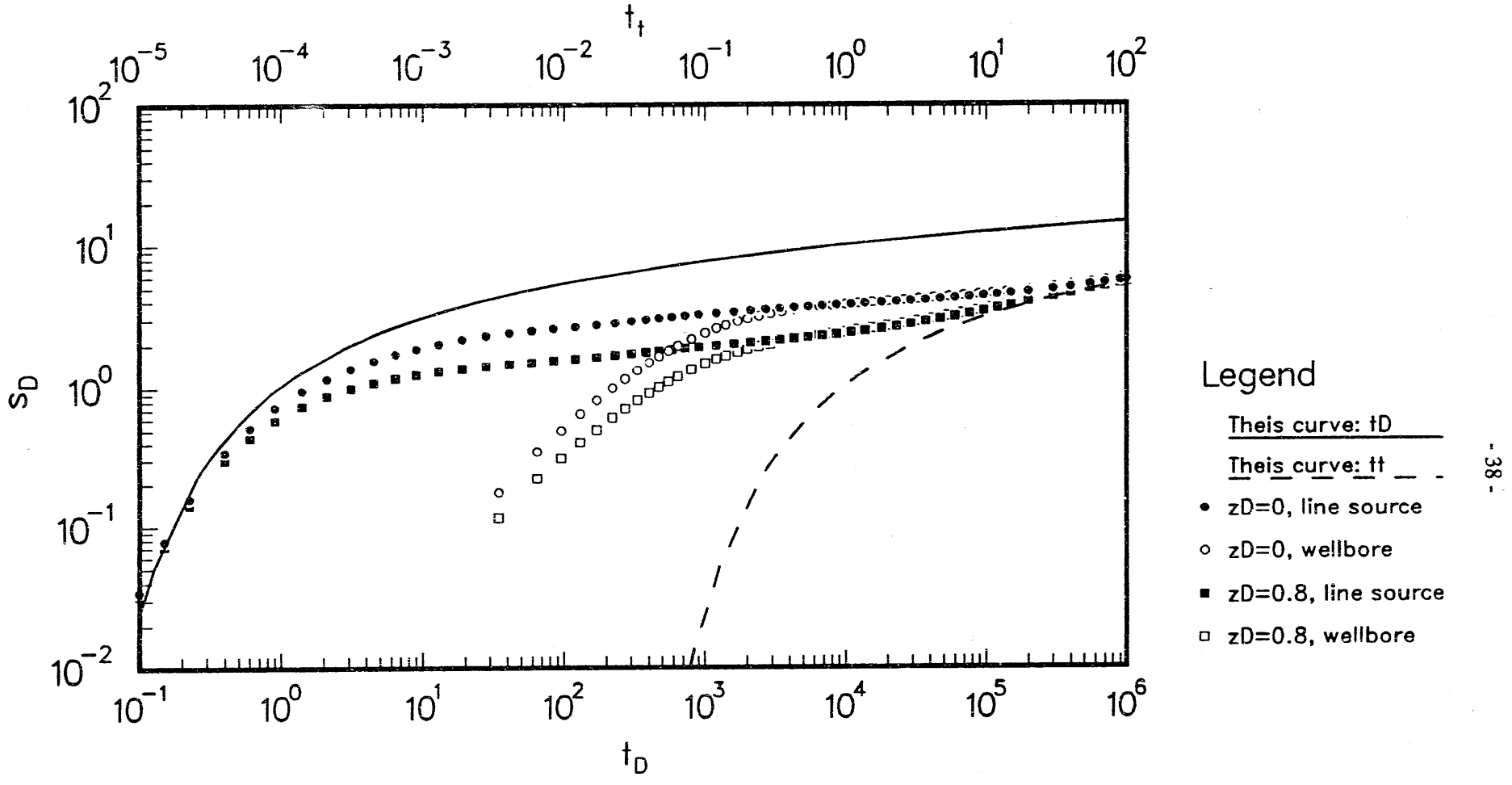

Fig. 11a. Neuman problem: Effect of radial distance on point drawdown.
$\sigma = 0.0001$, $\beta=0.01$, $r_w = 0.128$ m, $S_y = 0.23$.

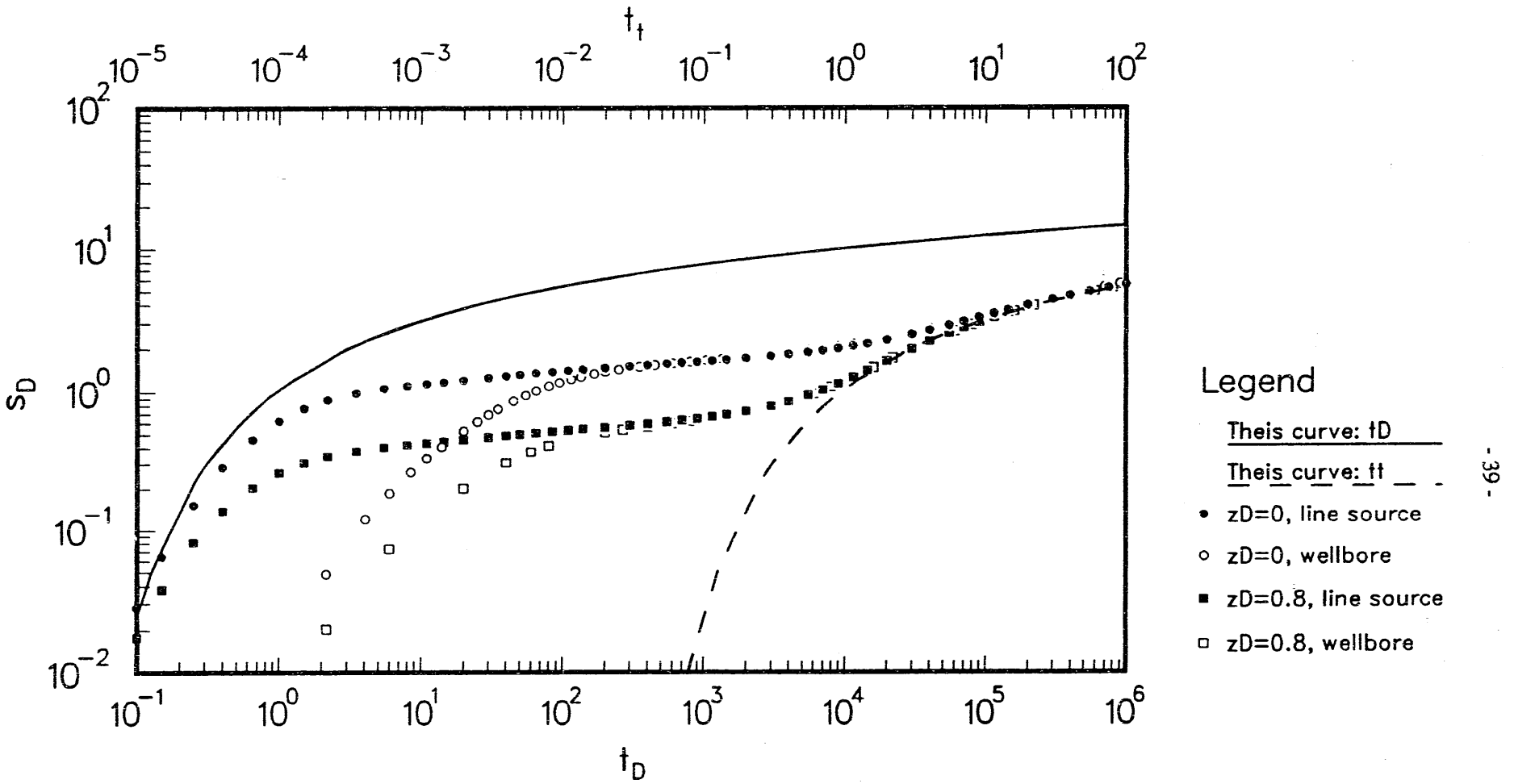

Fig. 11b. Neuman problem: Effect of radial distance on point drawdown.
σ = 0.0001, β=0.16, r_w = 0.128 m, S_y = 0.23.

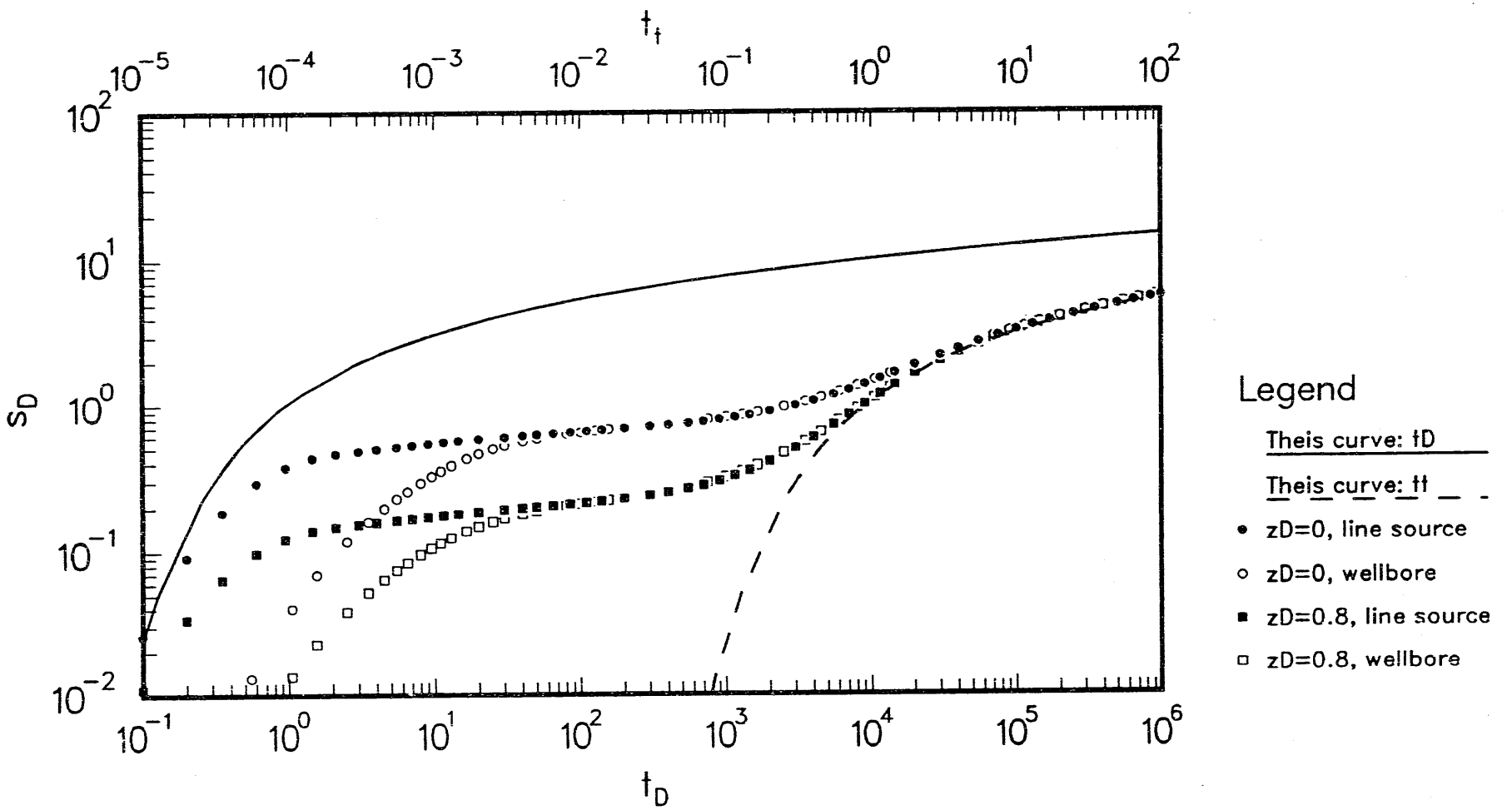

Fig. 11c. Neuman problem: Effect of radial distance on point drawdown.
σ = 0.0001, β=0.64, r_w = 0.128 m, S_y = 0.23.

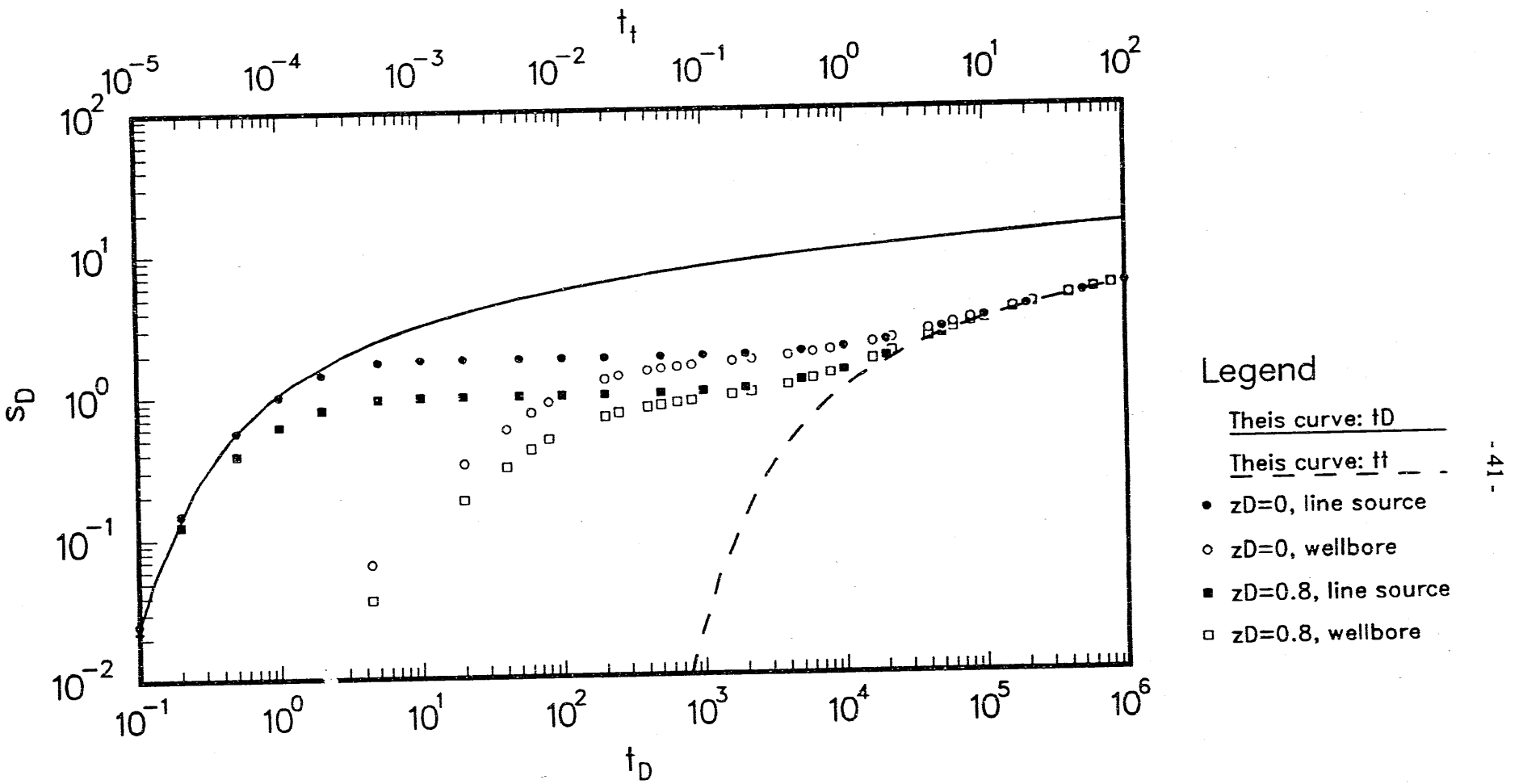

Fig. 11d. Neuman problem: Effect of radial distance on point drawdown.
$\sigma = 0.0001$, $\beta=0.16$, $r_w = 0.128$ m, $S_y = 0.115$.

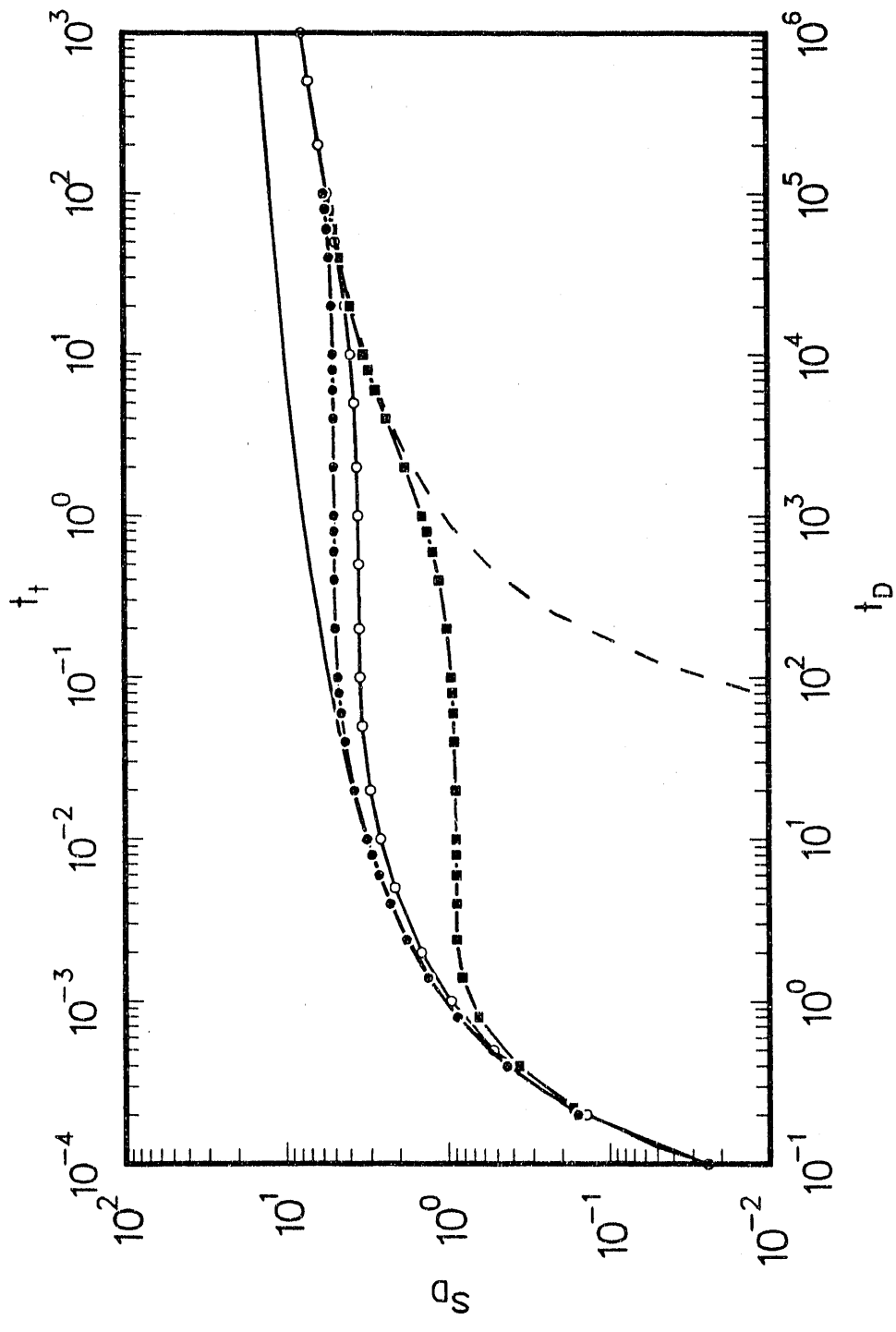

Fig. 12a. Comparison of Boulton model and Neuman model: σ=0.001, β=0.01.

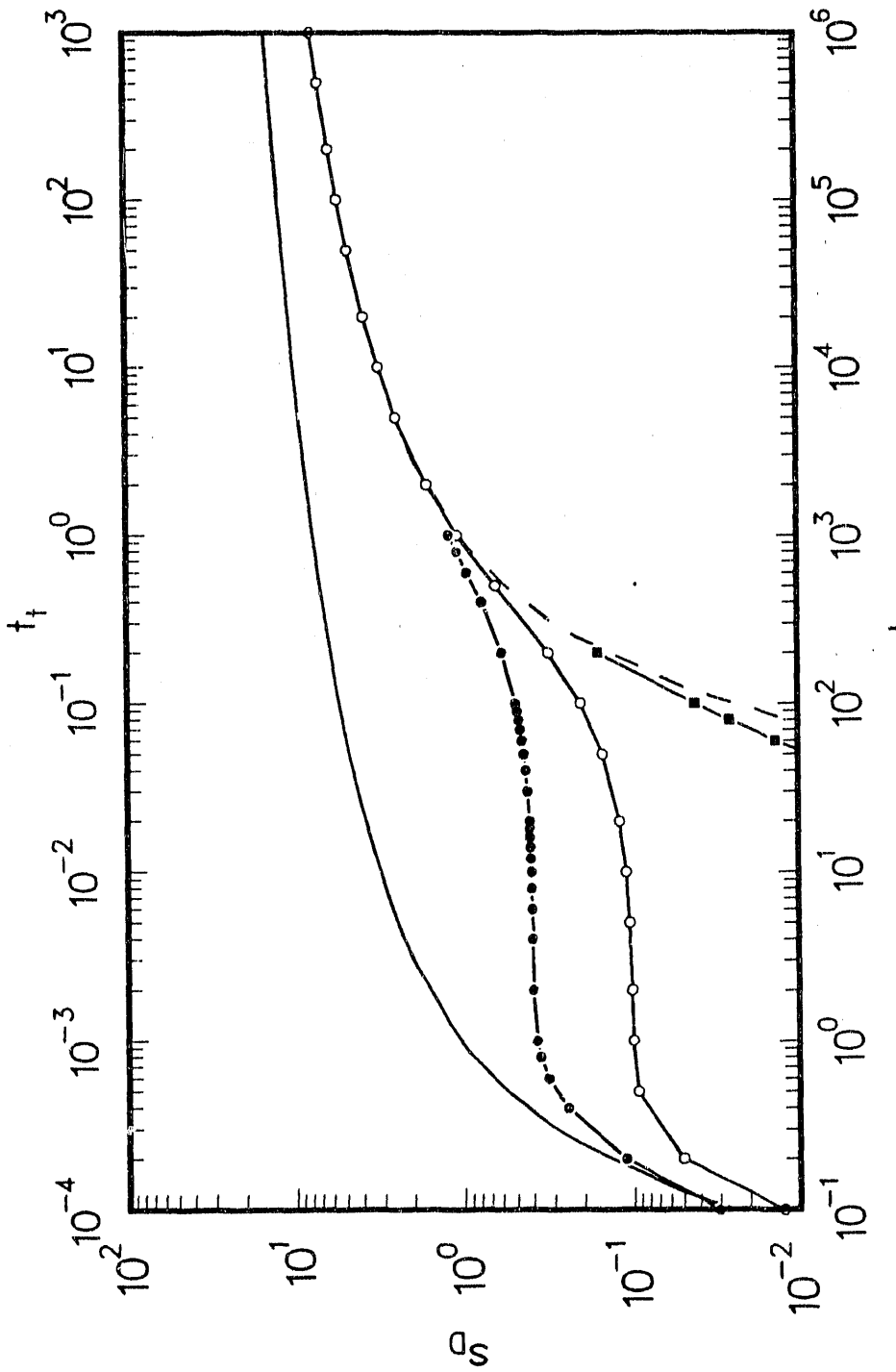

Fig. 12b. Comparison of Boulton model and Neuman model: σ=0.001, β=2.56.

END

DATE
FILMED
4 / 29 / 92